doi.org/10.26434/chemrxiv.9693506.v1

Ruthenium(II) Complexes Bearing Thioether-Appended α- Iminopyridine Ligands: Arene Precursors Permit Access to K2-N,N and K3-N,N,S Complexes

Victoria A. Ternes, Hannah A. Morgan, Austin P. Lanquist, Michael P. Murray, Bradley Wile

Submitted date: 20/08/2019 • Posted date: 21/08/2019

Citation information: Ternes, Victoria A.; Morgan, Hannah A.; Lanquist, Austin P.; Murray, Michael P.; Wile, Bradley (2019): Ruthenium(II) Complexes Bearing Thioether-Appended α- Iminopyridine Ligands: Arene Precursors Permit Access to K2-N,N and K3-N,N,S Complexes. ChemRxiv. Preprint.

Herein we report the preparation of a series of Ru(II) complexes featuring alpha-iminopyridine ligands bearing thioether functionality (NNS^{R}, where R = Me, CH_2Ph, Ph). Metallation using (p cymene)RuCl dimer permits access to (k^2-N,N)Ru complexes in which the thioether moiety remains uncoordinated. In the presence of a strong field ligand such as acetonitrile or triphenylphosphine, the p-cymene moiety is displaced, and the ligand adopts a k^3-N,N,S binding mode. These complexes are characterized using a combination of solution and solid state methods, including the crystal structure of $[(NNS^{Me})Ru(NCMe)_2Cl]Cl$. The k^2-N,N Ru(II) complexes are shown to serve as efficient precatalysts for the oxidation of sec-phenethyl alcohol at 5 mol% loadings, using a variety of external oxidants and solvents. The complex bearing an S-Ph donor was found to be the most active of those surveyed, suggesting that the thioether donor plays an active role in catalyst speciation for this transformation.

File list (2)

Ruthenium(II) complexes bearing thioether-appended α-iminopyridine ligands: Arene precursors permit access to κ^2-N,N and κ^3-N,N,S complexes

Ternes, Victoria A.; Morgan, Hannah A.; Lanquist, Austin P.; Murray, Michael J.; Wile, Bradley M.*

Donald J. Bettinger Department of Chemistry and Biochemistry, Ohio Northern University, 525 South Main Street, Ada, OH 45810, USA

ABSTRACT: Herein we report the preparation of a series of Ru(II) complexes featuring α-iminopyridine ligands bearing thioether functionality (NNS^R, where R = Me, CH_2Ph, Ph). Metallation using (*p*-cymene)RuCl dimer permits access to (κ^2-N,N)Ru complexes in which the thioether moiety remains uncoordinated. In the presence of a strong field ligand such as acetonitrile or triphenylphosphine, the *p*-cymene moiety is displaced, and the ligand adopts a κ^3-N,N,S binding mode. These complexes are characterized using a combination of solution and solid state methods, including the crystal structure of $[(NNS^{Me})Ru(NCMe)_2Cl]Cl$. The κ^2-N,N Ru(II) complexes are shown to serve as efficient precatalysts for the oxidation of *sec*-phenethyl alcohol at 5 mol% loadings, using a variety of external oxidants and solvents. The complex bearing an S-Ph donor was found to be the most active of those surveyed, suggesting that the thioether donor plays an active role in catalyst speciation for this transformation.

INTRODUCTION

Metal complexes bearing redox non-innocent ligands have continued to attract interest from organic and organometallic chemists.[1–8] Catalysts featuring a redox non-innocent ligand set frequently displayed enhanced activity relative to redox-innocent counterparts, particularly when base metals are employed.[9–13] Of this ligand class, α-iminopyridines are a robust and attractive redox-noninnocent framework, and they may be readily prepared from a wide range of commercially available reagents via the formation of a Schiff base.[14,15] Such redox-active ligands have been shown to support unprecedented metal-centered transformations, including alcohol oxidation,[16] water splitting,[17] nitrene transfer,[18] C-C bond formation,[19] hydrosilylation,[9,20] and hydrogenation.[3,21] This interest in redox-active ligand sets has spurred the development of new methodologies, and new ligands bearing additional donor atoms.

Several highly-active catalyst systems derived from di(imine) or α-imino(pyridine) have been reported in recent years.[22–27] For pre-catalysts derived from base metals, it is strongly implied that the redox-activity of these ligand sets confers stability by mitigating decomposition as a result of metal-centered one electron redox processes. Wieghardt and co-workers have explored the redox non-innocence of a wide variety of di(imine)[28–32] and α-imino(pyridine) complexes.[13,15,33–35] Using open shell, broken-symmetry DFT calculations, both di(imine) and α-imino(pyridine) complexes were found to contain low-lying π* systems that may accept one or two electrons, and α-imino(pyridine) complexes were also capable of donating electrons to a metal center from occupied ligand π orbitals. These findings suggest that the presence of a redox-innocent donor arm does not negate the activity of redox-active α-imino(pyridine) ligand frameworks. With these properties in mind, we sought to identify a series of ligands featuring a potentially redox-active moiety and a thioether donor, capable of selectively dechelating from the metal center. We imagine these species as useful pre-catalysts for a variety of transformations, and hoped to learn more about the solution chemistry of such complexes in order to better understand the origin of such catalyst activity.

While numerous ligands have been developed featuring P and N donors, less attention has been paid to other main group donors. Stradiotto and co-workers found that the inclusion of an oxygen donor led to a dramatic improvement in performance for the monoarylation of ammonia using Pd or Ni catalysts.[36–38] Inclusion of a soft thioether donor has been observed to generate ligands with greater air and moisture tolerance when compared to their phosphine counterparts, with properties that are highly tunable based on substitution of the thioether, or connectivity between the sulfur moiety and the amine donors.[39,40] A recent report by Phillips and co-workers describes the preparation and catalytic performance of Ru(II) arenes featuring β-thioketoiminates, a bidentate N,S analogue of the ubiquitous β-diketiminate (or "nacnac") ligands.[41] Ru(II) arene complexes featuring sulfur donors have also been shown to exhibit anticancer activity, wherein that activity is strongly influenced by the binding mode and oxidation state of the thiolate moiety.[42,43]

The presence of a third donor may also encourage the formation of more robust κ^3 complexes, relative to bidentate counterparts. Pd(II) and Ag(I) complexes bearing thioether-functionalized N-heterocyclic carbenes have been shown to demonstrate hemilability in the presence of moderate to strong donors such as phosphines.[44–46] Related reports by Huynh and co-workers describe a series of thioether-bridged diimidazolium dibromides that serve as precursors to κ^3-C,S,C (pincer) and κ^2-C,C (pseudo-pincer) Pd(II) complexes.[47,48] Encouragingly, these species bearing a hemilabile sulfur donor

were found to serve as efficient pre-catalysts for a variety of cross-coupling applications, suggesting that the traditional view of sulfur as a "catalyst poison" is not applicable in all instances. Similarly, Bianchini and co-workers found that the inclusion of a heterocyclic sulfur donor led to Co(II) catalysts with improved selectivity for the oligomerization of α-olefins when compared with α-imino(pyridine) counterparts.[49] Recent studies by Kovacs and co-workers suggests that inclusion of a thiolate donor in α-imino(N-heterocycle) ligands may stabilize base metal complexes through extensive involvement of the sulfur moiety in frontier orbitals.[50]

While several complexes featuring a thiol donor (i.e. R = H) are known, these compounds are also known to isomerize to form the corresponding benzothiazoline or benzothiazole, or to generate the corresponding disulfide.[51–55] Introduction of a thioether substituent blocks this tautomerization,[56–58] enabling the preparation of complexes of pmtpm (**1, Scheme 1**) featuring manganese,[59] iron,[60] cobalt,[56] nickel,[61,62] and ruthenium.[63,64] Early reports emphasized the structural homology between these complexes and the related metalloenzymes (e.g. [Ni-Fe] hydrogenase, plastocyanins, alcohol dehydrogenase),[65,66] while more recent work has explored the utility of such metal complexes as homogeneous catalysts,[49] or vessels for carbon monoxide delivery.[59,67] Given the broad range of metals supported by the class of ligands, we sought to identify well-defined catalytic processes that might benefit from the presence of a thioether donor.

Scheme 1. Preparation of pyridyl(thiophenyl-methyleneimine) ligands 1-3.

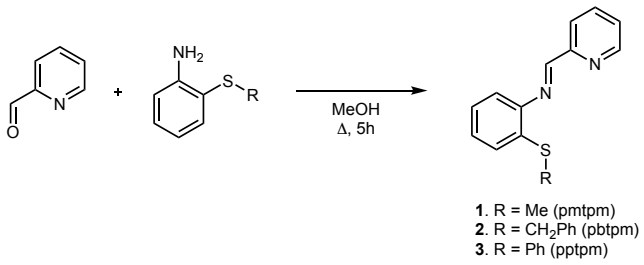

Selective oxidation of alcohols may be accomplished through the use of stoichiometric metal reagents, though methods with lower toxicity and reduced environmental impacts are preferred. The Ley-Griffith oxidation, employing tetra-N-propyl ammonium perruthenate (TPAP) in combination with N-methylmorpholine N-oxide (NMO) has been widely adopted because of the mild conditions and general functional group tolerance for this system, though mechanistic studies into this system are ongoing.[68–71] Structurally similar (NS) or (NN) complexes of ruthenium have been shown to serve as competent catalysts for alcohol oxidation, though the identity of the active catalyst and intermediate species are still debated.[72–74] These Ru-arene species are proposed to go through a Ru(IV)=O intermediate, with proposed partial or complete dissociation of the thioether ligand. Additional insight in the transformations of similar Ru complexes featuring thioether iminopyridine ligands may further elucidate the mechanism by which these transformations take place, allowing for more efficient catalyst design, and expansion of substrate scope. To this end, we report the synthesis and characterization of a series of Ru arene complexes featuring the thioether α-iminopyridine ligands **1-3**, as well as an evaluation of catalytic performance of these complexes for the oxidation of *sec*-phenethyl alcohol.

RESULTS AND DISCUSSION

Ligand and complex preparation. Ligands (**1-3**) were readily prepared from commercially-available thioether anilines and pyridine 2-carboxaldehyde. The Schiff base **3** was obtained as ivory needles using a standard reflux setup in methanol. In the solid state, ligand **3** is air sensitive, forming a yellow byproduct overnight. Under nitrogen atmosphere, the ivory solid is stable at room temperature, demonstrating mass spectral features (m/z = 291.0952, $[M + H]^+$) consistent with the formulation as **3**. Efforts to further characterize ligand **3** by solution NMR were hampered by facile cleavage of the imine to regenerate the pyridine-2-carboxaldehyde and 2-phenylthio-aniline. At 300K in acetone-d^6 solution, this cleavage is observed after approximately two hours in solution, permitting full characterization data to be obtained. A signal assigned to the imine C-H is observed at δ = 8.50, upfield of the corresponding aldehyde C–H in the pyridine-2-carboxaldehyde precursor. This upfield shift is indicative of the formation of the aldimine. Other signals attributed to the remaining 13 aromatic C–H residues are observed between 8.71 and 7.09 ppm, supporting the depiction of **3** (R = Ph) in scheme 2.

Scheme 2. Preparation of κ^2-(N,N) and κ^3-(N,N,S) Ru(II) complexes. i) 1.25 NH_4BF_4, MeOH, RT, 3h; ii) CH_3CN, 60ºC, 6h.

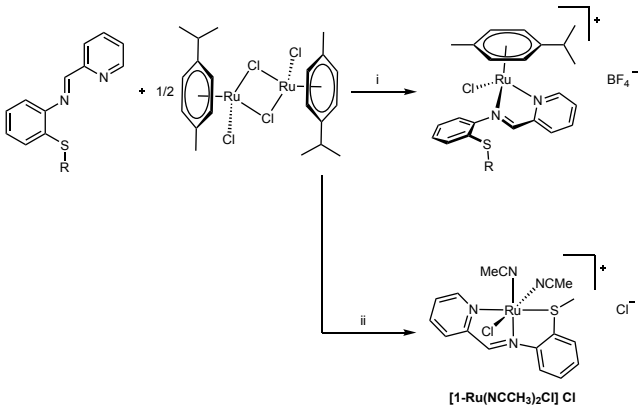

Metal complexes were prepared by stirring [Ru(*p*-cymene)Cl(μ-Cl)]$_2$ with the corresponding ligand (**1-3**) and ammonium tetrafluoroborate in methanol solution to afford the corresponding complex (Scheme 2) in moderate to excellent yield. The complexes **[1-Ru(*p*-cymene)Cl] BF_4** and **[2-Ru(*p*-cymene)Cl] BF_4** were isolated as dark green solids, while **[3-Ru(*p*-cymene)Cl] BF_4** was obtained as orange needles. The complexes were soluble in chloroform, acetone, acetonitrile, dimethylsulfoxide, and dichloromethane, and insoluble in diethyl ether, pentane, and water. Related complexes prepared in the absence of a non-coordinating anion (i.e., X = Cl) were not readily accessible in methanol, but could be prepared as a mixture of isomers by refluxing a mixture of the same metal precursor and the corresponding ligand (**1-3**) in dichloromethane solution under inert atmosphere. As observed for related ruthenium(II) complexes supported by α-iminopyridine ligands, all ruthenium species were sufficiently air stable to be handled under atmospheric conditions for routine manipulation and characterization, and not hygroscopic.[74] Samples of both **[1-Ru(*p*-cymene)Cl] BF_4** and **[3-Ru(*p*-cymene)Cl] BF_4** powders that were allowed stand at room temperature in screw-capped vials for extended periods (> approximately 6 months) with no further efforts to preclude

the admission of air or water were found to exhibit broadened and shifted ^{1}H NMR signals spectra consistent with the presence of a paramagnetic impurity. Aerobic oxidation to form a corresponding Ru(III) complex may be responsible for this observation, though efforts to isolate these species have been unsuccessful to date.

These Ru complexes were characterized by ^{1}H and ^{13}C NMR, with assignments confirmed through the use of two dimensional spectra. Limited solubility of **[1-Ru(*p*-cymene)Cl] BF_4** in $CDCl_3$ prevented complete characterization, though dilute samples showed clean ^{1}H spectral features consistent with those observed for **[2-Ru(*p*-cymene)Cl] BF_4** and **[3-Ru(*p*-cymene)Cl] BF_4**. ^{1}H NMR of **[1-Ru(*p*-cymene)Cl] BF_4** in DMSO-d^6 shows the expected number of signals, with clear separation between most resonances. A signal at δ = 8.95 attributed to the imine C–H is within the expected range for a coordinated aldimine.[56] Four distinct doublets, each integrating for one proton were observed upfield of the aromatic region (δ = 6.06, 5.81, 5.73, and 5.33), suggesting that the *p*-cymene residue is bound to the Ru center in an η^6 fashion, with front to back asymmetry. This formulation is further confirmed by the presence of two distinct *iso*-propyl CH_3 signals at δ = 1.04 and 0.97. ^{13}C{^{1}H} NMR of **[1-Ru(*p*-cymene)Cl] BF_4** in DMSO-d^6 shows similar complexity arising from a non-symmetrical *p*-cymene, with C–H signals at δ = 87.7, 87.2, 86.7, and 84.5. Similar spectral features are observed in $CDCl_3$ for **[2-Ru(*p*-cymene)Cl] BF_4** and **[3-Ru(*p*-cymene)Cl] BF_4**, notably the presence of four doublets between 5.0 and 6.0 ppm corresponding to four distinct *p*-cymene C–H environments and a singlet assigned to the aldimine C–H (δ = 7.90-7.75 for **[2-Ru(*p*-cymene)Cl] BF_4** and 8.13 for **[3-Ru(*p*-cymene)Cl] BF_4**) observed upfield of the corresponding aldehyde C–H. In the ^{1}H spectrum for **[2-Ru(*p*-cymene)Cl] BF_4**, a the signal assigned to the methylene group is observed at δ =4.25, suggesting that the thioether donor remains unbound, but near the Ru center such that an electrostatic interaction is possible without the formally diastereotopic signals expected if the S-donor had coordinated. Combined, these data support the assignment of a κ^2-N,N coordination mode for the Ru complexes of ligands **1-3** prepared in this manner.

Unlike previously reported Ru(II) complexes of pmtpm (**1**) in which κ^3-N,N,S coordination modes were observed,[63,64] the complexes reported here feature a κ^2-N,N coordination mode. This difference may be attributed to the use of the [Ru(*p*-cymene)Cl_2]$_2$ precursor, rather than $Ru(PPh_3)_3Cl_2$ as employed in other studies. While the arene complexes **[(NN)-Ru(*p*-cymene)Cl] BF_4** (NN = ligands **1** – **3**) are stable for extended periods in our hands, we postulated that loss of the arene ligand via ligand substitution might give rise to complexes in which these ligands adopt κ^3 coordination modes. To this end, addition of two equivalents of triphenylphosphine to a solution of **[1-Ru(*p*-cymene)Cl] BF_4** in $CDCl_3$ resulted in a rapid color change from dark green to purple upon heating at 70ºC for one hour. ^{1}H NMR of this solution revealed complete disappearance of signals attributed to Ru-bound arene C–Hs (δ = 5.81, 5.66, 5.58, and 5.29 ppm), while ^{31}P{^{1}H} NMR exhibited a new signal at δ = 17.40 consistent with the chemical shifts observed for related arene Ru(II) complexes.[75] Combined, these data suggest loss of the *p*-cymene ligand to form a complex such as **[1-Ru(PPh_3)$_2$Cl] BF_4** with two equivalent triphenylphosphine ligands, likely requiring a κ^3-N,N,S binding mode to complete the coordination sphere. Attempts to isolate and fully characterize this product resulted in decomposition. Although the putative **[1-Ru(PPh_3)$_2$Cl] BF_4** was precipitated from $CDCl_3$ solution by addition of copious Et_2O, ^{1}H and ^{31}P spectral features of this isolated solid in DMSO-d^6 solution suggest several phosphorus-containing species (δ = 50.33, 36.08, 17.40) are formed, likely as a result of solvation.[76,77] Notably, this complex is different from the **[1-Ru(PPh_3)Cl_2]** observed when **1** is heated in the presence of $Ru(PPh_3)_3Cl_2$ in benzene.[64]

Scheme 3. Synthesis of [1-Ru($NCCH_3$)$_2$Cl] Cl via solvation and loss of *p*-cymene.

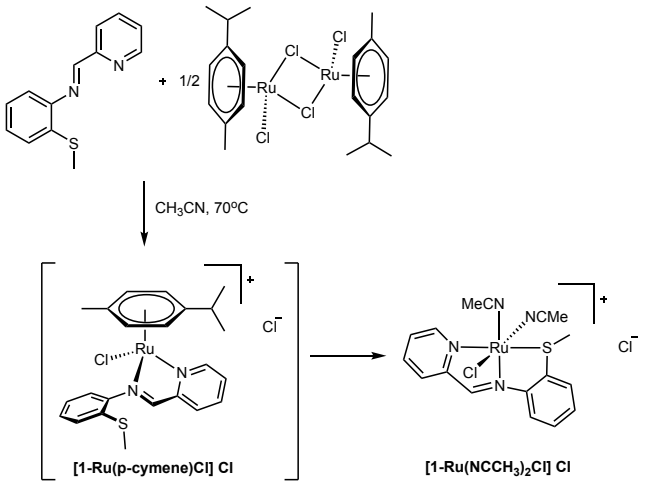

A related complex featuring an outer sphere chloride ligand was prepared by heating pmtpm (**1**) and one equivalent of [Ru(*p*-cymene)Cl(μ-Cl)]$_2$ in acetonitrile solution. The reaction mixture initially turned dark green, suggesting the presence of an intermediate complex of the formulation **[1-Ru(*p*-cymene)Cl] Cl**, which is gradually displaced over the course of ~3 hours to form a dark purple solution. The dark purple complex **[1-RuCl(NCMe)$_2$] Cl** was precipitated from solution by addition of diethyl ether in good yield. ^{1}H NMR of this complex in DMSO-d^6 solution reveals spectroscopic features consistent with those observed for the closely related **[1-Ru(*p*-cymene)Cl] BF_4**. The imine C-H resonance for **[1-RuCl(NCMe)$_2$] Cl** appears downfield (δ = 10.02) of that observed for **[1-Ru(*p*-cymene)Cl] BF_4** (δ = 8.95), suggesting that coordination of the thioether donor, or loss of the arene ligand significantly alters the magnetic environment of the imine moiety. Resonances attributed to bound acetonitrile (δ = 2.81, 2.75) are observed downfield of free acetonitrile. Combined, these data are consistent with the formulation **[1-RuCl(NCMe)$_2$] Cl** as shown in Scheme 3, in which the ligand has adopted a meridonal κ^3-N,N,S coordination mode as observed for related complexes **[1-Ru(PPh_3)Cl_2]**,[63,64] and the *p*-cymene ligand has been displaced in favor of two acetonitrile molecules.

The crystal structure of **[1-RuCl(NCMe)$_2$] Cl** was determined using single crystals grown from via slow evaporation of a saturated solution of the complex in acetonitrile solution (See Table S1 in the supporting information for crystallographic details). In the final structure, outer sphere chloride anions are disordered 1:1 with water molecules, and hydrogen bonding is observed between all three co-crystallized water molecules. The unit cell contains an inversion center that relates the two formula units, and short contacts are observed between adjacent Ru complexes (S1···S1 3.58 Å, H2···Cl1 2.67 Å, and H7···Cl1 2.53 Å). These interactions are close to the sum of the

van der Waals radii for the constituent atoms, suggesting that the structure is best considered as a discrete coordination complex rather than an extended network. The Ru1-Cl1 bond is consistent with reported lengths for Ru(II) complexes, and slightly shorter than the corresponding distances for **[1-Ru(PPh$_3$)Cl$_2$]**. The chloride counterion lies 5.492 Å from the Ru center, consistent with the depiction as an outer sphere anion. The Ru1-S1 bond is slightly longer (2.3137(5) Å) than reported for **[1-Ru(PPh$_3$)Cl$_2$]**, as expected due to the Ru1-S1-C13 bond angle of 111.89(8)°. Deviation from 90° implies poorer overlap of the S HOMO (nearly all 3p in character) with an unoccupied Ru orbital, thus weakening this bond.[78,79] Indeed, deviation from the ideal octahedral geometry is evidenced by the N1-Ru1-S1 angle of 164.52(5)°, as well as individual donor atom-Ru bond angles that differ significantly from 90° (N1-Ru1-N2 79.41(7)°; N2-Ru1-S1 85.40(5)°; S1-Ru1-N3 96.19(5)°; N1-Ru1-N3 98.94(7)°; N3-Ru1-N4 87.00(8)°). The ruthenium center is contained within the plane defined by N1-N2-N3-S1, deviating by 0.039 Å from the plane.

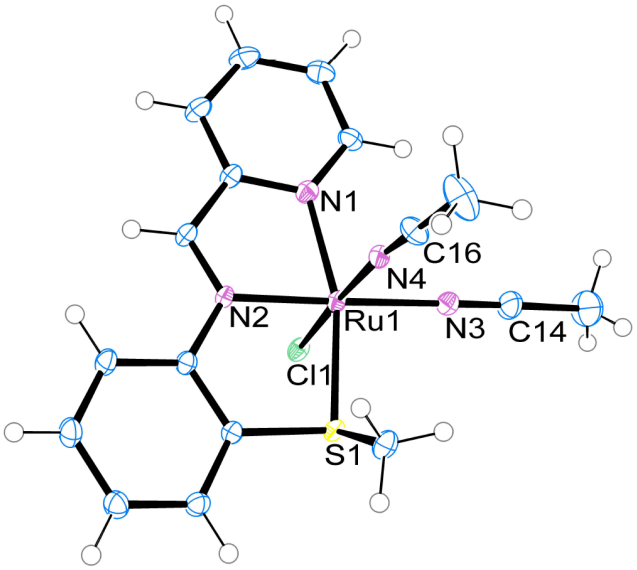

Figure 1. ORTEP depiction for **[1-RuCl(NCMe)$_2$] Cl** shown with 50% displacement ellipsoids and the numbering scheme for selected atoms shown. Hydrogen atoms are drawn arbitrarily small for clarity. Non-coordinating chloride ion and water molecules present from crystallization have been omitted for clarity. Selected bond distances (Å) and angles (°) for **[1-RuCl(NCMe)$_2$] Cl**: N1-Ru1 2.079(2); N2-Ru1 1.988(2); N3-Ru1 2.043(2); N3-C14 1.147(4); N4-Ru1 2.013(2); N4-C16 1.134(3); S1-Ru1 2.3137(5); Cl1-Ru1 2.4066(6); N1-Ru1-N2 79.41(7); N2-Ru1-S1 85.40(5); S1-Ru1-N3 96.19(5); N1-Ru1-N3 98.94(7); N3-Ru1-N4 87.00(8); N1-Ru1-S1 164.52(5).

Catalytic studies (alcohol oxidation). The lability of the *p*-cymene residue prompted further investigation of the ability for these complexes to serve as pre-catalysts for the oxidation of alcohols under mild conditions. The oxidation of *sec*-phenethyl alcohol to acetophenone was chosen as a model system which could be examined under mild conditions and easily analyzed using ^{1}H NMR spectra of reaction mixtures *in situ*. No conversion was observed in the absence of precatalyst (Table 1, entries 1-3). Using iodosylbenzene as the oxidant, all three Ru *p*-cymene complexes exhibited modest conversion after 30 minutes at 30°C in $CDCl_3$ solution, which rose after 24 hours (entries 4-9). Employing N-methylmorpholine N-oxide (NMO) as the oxidant under identical conditions, all three complexes displayed poorer conversion when compared with iodosylbenzene (entries 11-13). Similarly reduced conversion was noted when benzoyl peroxide was employed as the oxidant (entries 14-15), even with prolonged reaction times. Using the conditions found to promote the greatest conversion from this initial screen (entry 9, 58.1%), and increasing the quantity of oxidant from one to three molar equivalents resulted in full conversion to acetophenone over 24 hours (entry 10, >99%). A similar increase in conversion was noted with **[1-Ru(*p*-cymene)Cl] BF$_4$** when three equivalents of iodosylbenzene were employed (entry 20, 73.5%).

Using iodosylbenzene as the oxidant in combination with **[3-Ru(*p*-cymene)Cl] BF$_4$**, a broader solvent compatibility scope was undertaken. Employing three equivalents of isodosylbenzene, excellent conversions were noted in dichloromethane (entry 16, 94.3%), acetone (entry 17, >99%), and acetonitrile (entry 18, 98.4%). In acetonitrile solution, reduced conversion was noted when 5% NaOCl(*aq*) was employed as the oxidant (49.5%, entry 18), and no conversion was noted (entry 19) when 30% H_2O_2(*aq*) was employed as the oxidant. Combined, these data demonstrate that the ruthenium *p*-cymene complexes reported here serve as effective pre-catalysts for the oxidation of *sec*-phenethyl alcohol, across a broad range of solvents. While the mechanism by which these catalysts operate is unknown, the high conversions observed in coordinating solvents (entries 17 and 18), as well as the solvent-assisted loss of p-cymene to form **[1-RuCl(NCMe)$_2$] Cl** suggest that solvento adducts may play a critical role in the catalytic cycle, as observed for related Ley-Griffith (TPAP) catalyzed alcohol oxidation.[70,71]

Scheme 4. Oxidation of *sec*-phenethyl alcohol.

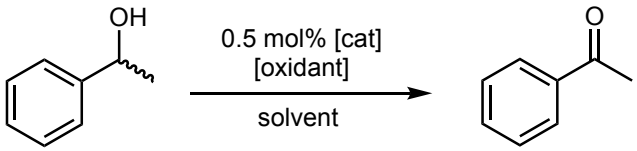

CONCLUSION

The complexes described here represent new binding modes for thioether-appended α-iminopyridine ligands on a Ru(II) center. These complexes demonstrate the potential for hemilabile binding of the NNS ligand, and serve as useful precatalysts for the oxidation of *sec*-phenethyl alcohol. The presence of both κ^2 and κ^3 binding modes suggest that the *p*-cymene complexes serve as masked forms of $[L_3Ru(II)Cl]^+$, in which two coordination sites are available for coordination of additional donors or substrates. While no redox-activity is observed in the complexes reported here, the presence of a thioether donor undoubtedly influences the coordination behavior of the Ru(II) center, relative to related α-iminopyridine ligands, as evidenced by the range of precatalyst activity for ligands bearing different thioether substitution. Further studies with related ligands using a mixed-donor (N,S) approach are ongoing in our laboratory, and will be reported in due course.

Table 1. Oxidation of *sec*-phenethyl alcohol by (κ^2-N,N)Ru(II) arene complexes.

Entry	Pre-catalyst	Oxidant	Solvent	Time (h)	% Conversion
1	none	PhIO	$CDCl_3$	24	n.d.
2	none	NMO	$CDCl_3$	24	n.d.
3	none	benzoyl peroxide	$CDCl_3$	24	n.d.
4	[1-Ru(*p*-cymene)Cl] BF_4	PhIO	$CDCl_3$	0.5	5.3
5	[1-Ru(*p*-cymene)Cl] BF_4	PhIO	$CDCl_3$	24	27.4
6	[2-Ru(*p*-cymene)Cl] BF_4	PhIO	$CDCl_3$	0.5	39.4
7	[2-Ru(*p*-cymene)Cl] BF_4	PhIO	$CDCl_3$	24	44.0
8	[3-Ru(*p*-cymene)Cl] BF_4	PhIO	$CDCl_3$	0.5	18.5
9	[3-Ru(*p*-cymene)Cl] BF_4	PhIO	$CDCl_3$	24	58.1
10	[3-Ru(*p*-cymene)Cl] BF_4	PhIO[a]	$CDCl_3$	24	>99
11	[1-Ru(*p*-cymene)Cl] BF_4	NMO	$CDCl_3$	24	16.7
12	[2-Ru(*p*-cymene)Cl] BF_4	NMO	$CDCl_3$	24	24.3
13	[3-Ru(*p*-cymene)Cl] BF_4	NMO	$CDCl_3$	24	5.9
14	[1-Ru(*p*-cymene)Cl] BF_4	benzoyl peroxide	$CDCl_3$	96	7.6
15	[3-Ru(*p*-cymene)Cl] BF_4	benzoyl peroxide	$CDCl_3$	24	26.9
16	[3-Ru(*p*-cymene)Cl] BF_4	PhIO[a]	CH_2Cl_2	24	94.3
17	[3-Ru(*p*-cymene)Cl] BF_4	PhIO[a]	acetone	24	>99
18	[3-Ru(*p*-cymene)Cl] BF_4	PhIO[a]	acetonitrile	24	98.4
18	[3-Ru(*p*-cymene)Cl] BF_4	NaOCl[a]	acetonitrile	24	49.5
19	[3-Ru(*p*-cymene)Cl] BF_4	H_2O_2[a]	acetonitrile	24	n.d.
20	[1-Ru(*p*-cymene)Cl] BF_4	PhIO[a]	acetonitrile	24	73.5

EXPERIMENTAL SECTION

General Considerations. High purity reagents and solvents were purchased from Sigma-Aldrich Ltd., Acros Organics, or Strem Chemicals Inc., and were used without further purification unless otherwise noted. Ligands **1**[56] and **2**[58] were prepared using reported literature procedures. Unless specifically noted, manipulations were conducted under inert atmosphere using standard air-free techniques. All products were characterized by ^{1}H and ^{13}C{^{1}H} NMR, with peak assignments assisted by the use of DEPT-135, ^{1}H-^{13}C HSQC, and ^{1}H-^{13}C HMBC experiments. NMR spectra were recorded on a Bruker Avance 400 spectrometer using a BBO probe operating at 400.1325 MHz (^{1}H) or 100.6208 MHz (^{13}C). Chemical shifts are reported in ppm downfield of $SiMe_4$, and referenced using the solvent residual peak. IR spectra were recorded on a Thermo Nicolet 6700 FTIR spectrometer as KBr pellets. Elemental analyses (C, H, N) were conducted by Midwest Microlab, LLC in Indianapolis, IN. Single crystal X-ray diffraction data were collected at 100K using a Bruker AXS D8 Quest CMOS diffractometer at Purdue University in West Lafayette, IN. Experimental data for compounds characterized by single crystal X-ray diffraction studies are summarized in Table S1.

Preparation of 2-(phenylthio)phenyl)-1-(2-pyridyl)methylimine (3) 2-(phenylthio)aniline (2.112 g, 10.49 mmol) was placed in a 250 mL round bottomed flask equipped with a PTFE coated stir bar, and dissolved in 75 mL of reagent grade methanol. Pyridine-2-carboxaldehyde (1.00 mL, 10.5 mmol) was added dropwise, and the solution was brought to reflux under atmospheric conditions. After 24 h, the solution was allowed to cool to room temperature, and approximately half of the solvent (and other volatiles) was removed in vacuo. This concentrated solution was placed in the freezer to yield the product (**3**) as ivory needles (3.070 g, 10.36 mmol, 99%). ^{1}H NMR (acetone-d^6) δ = 8.71 (d, $^3J_{HH}$ = 4.8 Hz, 1H, py), 8.50 (s, 1H, imine C-H), 8.21 (d, $^3J_{HH}$ = 8.0 Hz, 1H, CH), 7.94 (t, $^3J_{HH}$ = 8.0 Hz, 1H, py), 7.54-7.48 (m, 1H, CH), 7.47-7.32 (m, 6H, CH), 7.28-7.17 (m, 2H, CH), 7.09 (dd, $^3J_{HH}$ = 8.0 Hz, $^4J_{HH}$ = 1.2, 1H, CH). ^{13}C{^{1}H} NMR (acetone-d^6) δ = 156.0 (4°), 148.4 (CH), 147.4 (4°), 137.1 (CH), 136.7 (4°), 131.2 (CH), 128.9 (CH), 127.6 (CH), 125.8 (CH), 123.6 (CH), 122.5 (CH), 118.2 (CH), 115.8 (4°), 112.9 (CH), 83.3 (imine CH). mp 73-77 °C. IR (KBr, cm^{-1}) 3051, 2969, 1476, 1462, 1060, 772, 752. HRMS (M/Z, ESI+) expected for $[M + H]^+$: 291.0950; found: 291.0952.

Preparation of [1-Ru(p-cymene)Cl] BF_4 2-(methylthio)phenyl)-1-(2-pyridyl)methylimine (**1**, 151.6 mg, 0.66 mmol), di-μ-chlorobis[(*p*-cymene)chlororuthenium(II) dimer (202.2 mg, 0.33 mmol, 1 eq Ru), and ammonium tetrafluoroborate (102.7 mg, 0.98 mmol, 1.5 eq) were suspended in 15 mL dry methanol in a 20 mL scintillation vial, and stirred at room temperature for 3 h. The reaction volume was reduced in vacuo to approximately 8 mL, and 5 mL of dry Et_2O was added to facilitate precipitation. The red brown solid was filtered and rinsed with 5 mL of dry Et_2O, and the resulting product was allowed to dry under vacuum overnight to yield **[1-Ru(*p*-cymene)Cl] BF_4** (170.0 mg, 0.29 mmol, 88 %). ^{1}H NMR ($(CD_3)_2SO$) δ = 9.68 (d, $^3J_{HH}$ = 5.6 Hz, 1H, py), 8.95 (s, 1H, imine C-H), 8.35 (m, 2H, py), 7.98 (m, 1H, py), 7.72-7.67 (m, 2H, aryl C-H), 7.58 (t, $^3J_{HH}$ = 7.2 Hz, 1H, aryl C-H), 7.45 (t, $^3J_{HH}$ = 7.6 Hz, 1H, aryl C-H), 6.06 (d, $^3J_{HH}$ = 6.4 Hz, 1H, *p*-cymene aryl-H), 5.80 (d, $^3J_{HH}$ = 6.0 Hz, 1H, *p*-cymene aryl-H), 5.72 (d, $^3J_{HH}$ = 6.0 Hz, 1H, *p*-cymene aryl-H), 5.32 (d, $^3J_{HH}$ = 6.0 Hz, 1H, *p*-cymene aryl-H), 2.72-2.60 (m, 4H, CH_3 and *i*Pr CH), 2.11 (s, 3H, CH_3), 1.03 (d, $^3J_{HH}$ = 6.8 Hz, 1H, *i*Pr CH_3), 0.97 (d, $^3J_{HH}$ = 6.8 Hz, 1H, *i*Pr CH_3). ^{13}C{^{1}H} NMR ($(CD_3)_2SO$) δ = 156.7 (4°), 154.4 (4°), 150.2 (4°), 140.8 (CH), 130.9 (CH), 130.0 (CH), 129.6 (CH), 127.9 (CH), 126.2 (CH), 123.5 (CH), 106.7 (4°), 102.0 (4°), 87.7 (*p*-cymene aryl-CH), 87.2 (*p*-cymene aryl-CH), 86.7 (*p*-cymene aryl-CH), 84.5 (*p*-cymene aryl-CH), 31.0 (CH), 22.4 (CH_3), 21.8 (CH_3), 18.7 (CH_3), 16.1 (CH_3). mp 149 °C (decomp.). IR (KBr, cm^{-1}) 2960, 2927, 1465, 1437, 1066, 774. Anal. (%) calcd for $C_{23}H_{26}N_2BClF_4RuS$: C, 47.15; H, 4.47; N, 4.78. Found: C, 46.95; H, 4.44; N, 4.83.

Preparation of [2-Ru(p-cymene)Cl] BF_4 2-(benzylthio)phenyl)-1-(2-pyridyl)methylimine (**2**, 274 mg, 0.90 mmol), di-μ-chlorobis[(*p*-cymene)chlororuthenium(II) dimer (268 mg, 0.44 mmol, 1 eq. Ru), and ammonium tetrafluoroborate (122 mg, 1.16 mmol, 1.3 eq.) were

suspended in 15 mL dry methanol in a 20 mL scintillation vial, and stirred at room temperature for 16 h. The reaction mixture was placed in a freezer (-5°C) for 24 hours to facilitate precipitation of the crystalline product as a dark green to drab solid. The solid was filtered and rinsed with 5 mL dry Et_2O, and the resulting solid was allowed to dry in a vacuum desiccator to yield **[2-Ru(*p*-cymene)Cl] BF_4** (210 mg, 0.32 mmol, 35 %). ^{1}H NMR ($CDCl_3$) δ = 9.64 (d, $^3J_{HH}$ = 4.4 Hz, 1H, py), 8.06 (t, $^3J_{HH}$ = 7.2 Hz, 1H, aryl C-H), 7.90-7.75 (m, 4H, aryl C-H and imine C-H), 7.50 (t, $^3J_{HH}$ = 7.6 Hz, 1H, aryl C-H), 7.43-7.30 (m, 5H, aryl C-H), 7.17 (m, 2H, aryl C-H), 5.76 (d, $^3J_{HH}$ = 5.6 Hz, 1H, *p*-cymene aryl-H), 5.51 (d, $^3J_{HH}$ = 6.0 Hz, 1H, *p*-cymene aryl-H), 5.38 (d, $^3J_{HH}$= 5.6 Hz, 1H, *p*-cymene aryl-H), 5.23 (d, $^3J_{HH}$ = 6.0 Hz, 1H, *p*-cymene aryl-H), 4.25 (m, 2H, CH_2), 2.74 (septet, $^3J_{HH}$ = 6.8 Hz, 1H, ^{i}Pr CH), 2.14 (s, 3H, CH_3), 1.05 (d, $^3J_{HH}$ = 6.8 Hz, 3H, ^{i}Pr CH_3), 1.01 (d, $^3J_{HH}$ = 6.8 Hz, 3H, ^{i}Pr CH_3). ^{13}C{^{1}H} NMR ($CDCl_3$) δ = 196.4 (imine CH), 157.5 (aryl-CH), 153.1 (4°), 152.2 (4°), 139.5 (aryl-CH), 136.9 (aryl-CH), 131.8 (aryl-CH), 130.5 (aryl-CH), 129.8 (aryl-CH), 129.7 (aryl-CH), 129.2 (aryl-CH), 129.0 (aryl-CH), 128.7 (aryl-CH), 128.2 (aryl-CH), 127.9 (aryl-CH), 126.3 (aryl-CH), 126.2 (aryl-CH), 124.0 (aryl-CH), 108.7 (4° *p*-cymene α to ^{i}Pr), 102.0 (4° *p*-cymene α to CH_3), 87.3 (*p*-cymene aryl-CH), 86.5 (*p*-cymene aryl-CH), 86.3 (*p*-cymene aryl-CH), 84.1 (*p*-cymene aryl-CH), 40.1 (CH_2), 31.1(^{i}Pr CH), 22.2 (^{i}Pr CH_3), 22.0 (^{i}Pr CH_3), 18.7 (CH_3). mp 144 °C (decomp.). IR (KBr, cm^{-1}) 2966, 1472, 1084, 1065, 706. Anal. (%) calcd for $C_{29}H_{30}N_2BClF_4RuS$: C, 52.62; H, 4.57; N, 4.23. Found: C, 52.44; H, 4.64; N, 4.31.

Preparation of [3-Ru(p-cymene)Cl] BF_4 2-(phenylthio)phenyl)-1-(2-pyridyl)methylimine (**3**, 97 mg, 0.33 mmol), di-μ-chlorobis[(*p*-cymene)chlororuthenium(II) dimer (100 mg, 0.16 mmol, 1 eq. Ru), and ammonium tetrafluoroborate (46 mg, 0.44 mmol, 1.3 eq.) were suspended in 15 mL dry methanol in a 20 mL scintillation vial, and stirred at room temperature for 3 h. The reaction mixture was placed in a freezer (-5°C) for 24 hours to facilitate precipitation of the crystalline product as orange needles. The solid was filtered and rinsed with 5 mL dry Et_2O, and the resulting solid was allowed to dry in a vacuum desiccator to yield **[3-Ru(*p*-cymene)Cl] BF_4** (94 mg, 0.14 mmol, 43 %). ^{1}H NMR ($CDCl_3$) δ = 9.75 (d, $^3J_{HH}$ = 5.6 Hz, 1H, py), 8.13 (s, 1H, CH=N), 8.07 (t, $^3J_{HH}$ = 7.6 Hz, 1H, py), 8.03 - 7.93 (m, 2H, aryl-H), 7.83 (d, $^3J_{HH}$ = 7.2 Hz, 1H, py), 7.49 - 7.32 (m, 8H, aryl-H), 5.95 (d, $^3J_{HH}$ = 6.0 Hz, 1H, *p*-cymene aryl-H_a), 5.69 (d, $^3J_{HH}$ = 6.0 Hz, 1H, *p*-cymene aryl-H_b), 5.56 (d, $^3J_{HH}$ = 6.0 Hz, 1H, *p*-cymene aryl-H_c), 5.37 (d, $^3J_{HH}$ = 6.0 Hz, 1H, *p*-cymene aryl-H_d), 2.84 (septet, $^3J_{HH}$ = 6.8 Hz, 1H, *i*-Pr CH), 2.24 (s, 3H, *p*-cymene CH_3), 1.15 - 1.03 (m, 6H, *i*-Pr CH_3). ^{13}C{^{1}H} NMR ($CDCl_3$) δ = 169.6 (imine-CH), 157.8 (aryl-CH), 153.2 (4°), 151.4 (4°), 139.6 (py-CH), 132.9 (4°), 132.6 (aryl-CH), 131.5 (aryl-CH), 130.8 (aryl-CH), 130.2 (aryl-CH), 130.0 (aryl-CH), 129.9 (py-CH), 128.8 (aryl-CH), 128.4 (aryl-CH), 124.5 (aryl-CH), 108.7 (4°), 102.6 (4°), 87.1 (*p*-cymene aryl-CH_d), 86.9 (*p*-cymene aryl-CH_a), 86.3 (*p*-cymene aryl-CH_b), 84.4 (*p*-cymene aryl-CH_c), 31.2 (*i*-Pr CH), 22.2 (*i*-Pr CH_3), 22.0 (*i*-Pr CH_3), 18.9 (*p*-cymene CH_3). mp 168°C (decomp.). IR (KBr, cm^{-1}) 2968, 1476, 1457, 1060, 772, 752. Anal. (%) calcd for $C_{28}H_{28}N_2BClF_4RuS$: C, 51.90; H, 4.36; N, 4.32. Found: C, 50.96; H, 4.62; N, 4.23.

Preparation of [1-Ru(NCMe)$_2$Cl] Cl 2-(methylthio)phenyl)-1-(2-pyridyl)methylimine (**1**, 56 mg, 0.24 mmol) and di-μ-chlorobis[(*p*-cymene)chlororuthenium(II) dimer (74 mg, 0.12 mmol, 1 eq. Ru) were suspended in 10 mL spectroscopic grade acetonitrile in a 20 mL scintillation vial, and placed in an aluminum heating block at 70°C. Over the course of 3 hours, the reaction mixture turned green, then dark purple. After 6 hours had elapsed, the reaction mixture was cooled to room temperature and 10 mL diethyl ether was added. The capped vial was placed in a freezer (-5°C) for 24 hours to facilitate precipitation of the crystalline product as a purple microcrystalline solid. The solid was filtered and rinsed with 5 mL dry Et_2O, and the resulting solid was allowed to dry in a vacuum desiccator to yield ***[1-Ru(NCMe)$_2$Cl] Cl*** (54 mg, 0.11 mmol, 46 %). ^{1}H NMR ($CDCl_3$) δ = 10.02 (s, 1H, CH=N), 9.22 (d, $^3J_{HH}$ = 4.8 Hz, 1H, py), 8.39 (d, 1H, $^3J_{HH}$ = 8.0 Hz, aryl-H), 8.29 (d, $^3J_{HH}$ = 7.2 Hz, 1H, py), 8.21 (td, $^3J_{HH}$ = 7.6 Hz, $^4J_{HH}$ = 1.2 Hz, 1H, py), 8.11 (d, $^3J_{HH}$ = 7.2 Hz, 1H, aryl-H), 7.86 (td, $^3J_{HH}$ = 7.6 Hz, $^4J_{HH}$ = 1.2 Hz, 1H, py), 7.74 – 7.62 (m, 2H, aryl-H), 2.81 (s, 3H, CH_3CN), 2.75 (s, 3H, CH_3CN), 2.30 (s, 3H, S-CH_3). ^{13}C{^{1}H} NMR ($CDCl_3$) δ = 161.8 (4°), 159.8 (4°), 152.9 (imine-CH), 138.2 (CH), 133.0 (4°), 132.6 (CH), 130.3 (CH), 130.0 (CH), 128.6 (C≡N), 128.4 (CH), 117.8 (CH), 4.49 (*C*H_3CN), 3.80 (S-CH_3). mp >300°C. IR (KBr, cm^{-1}) 3428, 3351, 3010, 1597, 1476, 1436, 1419, 778, 746. Anal. (%) calcd for $C_{17}H_{18}N_4Cl_2RuS{\cdot}3H_2O$: C, 38.05; H, 4.51; N, 10.45. Found: C, 37.56; H, 4.63; N, 9.86.

General conditions for alcohol oxidation. Initial screening was conducted by combining *sec*-phenethyl alcohol (0.50 mmol), oxidant (0.50 mmol), and the appropriate catalyst (0.025 mmol) in 1.0 mL $CDCl_3$ in a borosilicate glass NMR tube. The tube was placed in a 30ºC bath, and monitored *in situ* at 0.5 h, 3 h, and 24 h by ^{1}H NMR. Further studies with other solvents were conducted in a 10 mL disposable glass vial fitted with a PTFE-lined pressure relief cap charged with magnetic stir bar, *sec*-phenethyl alcohol (0.50 mmol), oxidant (0.50 mmol) in the solvent (0.5 mL). A separate solution containing the catalyst (0.025 mmol) in 0.5 mL solvent was added to the alcohol mixture, and the vial was placed in an aluminum heating block set at 30ºC. After 24 hours (see Table 1), the reaction mixture was filtered through a pasteur pipette containing ~1 cm^3 of silica to remove the catalyst and quench any radical species. For reactions using bleach or hydrogen peroxide as the oxidant, the reaction mixture was also dried using $MgSO_4$ prior to filtering through silica. Percent conversion was determined using ^{1}H NMR spectroscopy by comparing integrated areas corresponding to the methyl peaks for *sec*-phenethyl alcohol (1.49 ppm), and acetophenone (2.59 ppm).

ASSOCIATED CONTENT

Supporting Information

Crystallographic data for **[1-RuCl(NCMe)$_2$] Cl** are available via the Cambridge Database (CCDC deposition number 1948202). These data can be obtained free of charge via www.ccdc.cam.ac.uk/data_request/cif, or by emailing data_request@ccdc.cam.ac.uk, or by contacting The Cambridge Crystallographic Data Centre, 12 Union Road, Cambridge CB2 1EZ, UK; fax: +44 1223 336033.

AUTHOR INFORMATION

Corresponding Author

* Bradley Wile b-wile@onu.edu (419) 772-2986

Notes

The authors declare no competing financial interest.

ACKNOWLEDGMENT

Funding for this research was provided by the American Chemical Society Petroleum Research Fund (#56549-UR3) and the Getty College of Arts and Sciences at Ohio Northern University, including a Ruth E. Weir summer research fellowship for APL. Matthias Zeller acquired single crystal data at Purdue University. Crystallographic facilities at Purdue University are supported under an NSF MRI grant (#CHE-1625543). David Blauch collected mass spectroscopy data for **3** at Davidson College, using an instrument acquired under an NSF MRI grant (#CHE-1624377).

REFERENCES

(1) Chirik, P. J. Preface: Forum on Redox-Active Ligands. *Inorg. Chem.* **2011**, *50* (20), 9737–9740.

(2) Kaim, W. Manifestations of Noninnocent Ligand Behavior. *Inorg. Chem.* **2011**, *50* (20), 9752–9765.

(3) Chirik, P. J. Iron- and Cobalt-Catalyzed Alkene Hydrogenation: Catalysis with Both Redox-Active and Strong Field Ligands. *Acc. Chem. Res.* **2015**, *48* (6), 1687–1695.

(4) Pattenaude, S. A.; Mullane, K. C.; Schelter, E. J.; Ferrier, M. G.; Stein, B. W.; Bone, S. E.; Lezama Pacheco, J. S.; Kozimor, S. A.; Fanwick, P. E.; Zeller, M.; et al. Redox-Active vs Redox-Innocent: A Comparison of Uranium Complexes Containing Diamine Ligands. *Inorg. Chem.* **2018**, *57* (11), 6530–6539.

(5) Luca, O. R.; Crabtree, R. H. Redox-Active Ligands in Catalysis. *Chem. Soc. Rev.* **2013**, *42* (4), 1440–1459.

(6) Eisenberg, R.; Gray, H. B. Noninnocence in Metal Complexes: A Dithiolene Dawn. *Inorg. Chem.* **2011**, *50* (20), 9741–9751.

(7) Praneeth, V. K. K.; Ringenberg, M. R.; Ward, T. R. Redox-Active Ligands in Catalysis. *Angew. Chemie Int. Ed.* **2012**, *51* (41), 10228–10234.

(8) Chirik, P. J.; Wieghardt, K. Radical Ligands Confer Nobility on Base-Metal Catalysts. *Science* **2010**, *327* (5967), 794–795.

(9) Tondreau, A. M.; Atienza, C. C. H.; Weller, K. J.; Nye, S. A.; Lewis, K. M.; Delis, J. G. P.; Chirik, P. J. Iron Catalysts for Selective Anti-Markovnikov Alkene Hydrosilylation Using Tertiary Silanes. *Science* **2012**, *335* (6068), 567–570.

(10) Lyaskovskyy, V.; de Bruin, B. Redox Non-Innocent Ligands: Versatile New Tools to Control Catalytic Reactions. *ACS Catal.* **2012**, *2* (2), 270–279.

(11) Ringenberg, M. R.; Nilges, M. J.; Rauchfuss, T. B.; Wilson, S. R. Oxidation of Dihydrogen by Iridium Complexes of Redox-Active Ligands. *Organometallics* **2010**, *29* (8), 1956–1965.

(12) Stubbert, B. D.; Peters, J. C.; Gray, H. B. Rapid Water Reduction to H2 Catalyzed by a Cobalt Bis(Iminopyridine) Complex. *J. Am. Chem. Soc.* **2011**, *133* (45), 18070–18073.

(13) Lu, C. C.; Bill, E.; Weyhermüller, T.; Bothe, E.; Wieghardt, K. Neutral Bis(α-Iminopyridine)Metal Complexes of the First-Row Transition Ions (Cr, Mn, Fe, Co, Ni, Zn) and Their Monocationic Analogues: Mixed Valency Involving a Redox Noninnocent Ligand System. *J. Am. Chem. Soc.* **2008**, *130* (10), 3181–3197.

(14) Blay, G.; Climent, E.; Fernández, I.; Hernández-Olmos, V.; Pedro, J. R. Enantioselective Henry Reaction Catalyzed with Copper(II)–Iminopyridine Complexes. *Tetrahedron: Asymmetry* **2007**, *18* (13), 1603–1612.

(15) Lu, C. C.; George, S. D.; Weyhermüller, T.; Bill, E.; Bothe, E.; Wieghardt, K. An Electron-Transfer Series of High-Valent Chromium Complexes with Redox Non-Innocent, Non-Heme Ligands. *Angew. Chemie Int. Ed.* **2008**, *47* (34), 6384–6387.

(16) Gunanathan, C.; Ben-David, Y.; Milstein, D. Direct Synthesis of Amides from Alcohols and Amines with Liberation of H_2. *Science* **2007**, *317* (5839), 790–792.

(17) Kohl, S. W.; Weiner, L.; Schwartsburd, L.; Konstantinovski, L.; Shimon, L. J. W.; Ben-David, Y.; Iron, M. A.; Milstein, D. Consecutive Thermal H_2 and Light-Induced O_2 Evolution from Water Promoted by a Metal Complex. *Science* **2009**, *324* (5923), 74–77.

(18) Nguyen, A. I.; Zarkesh, R. A.; Lacy, D. C.; Thorson, M. K.; Heyduk, A. F. Catalytic Nitrene Transfer by a Zirconium(IV) Redox-Active Ligand Complex. *Chem. Sci.* **2011**, *2* (1), 166–169.

(19) Haneline, M. R.; Heyduk, A. F. C−C Bond-Forming Reductive Elimination from a Zirconium(IV) Redox-Active Ligand Complex. *J. Am. Chem. Soc.* **2006**, *128* (26), 8410–8411.

(20) Trovitch, R. J. The Emergence of Manganese-Based Carbonyl Hydrosilylation Catalysts. *Acc. Chem. Res.* **2017**, *50* (11), 2842–2852.

(21) Friedfeld, M. R.; Shevlin, M.; Hoyt, J. M.; Krska, S. W.; Tudge, M. T.; Chirik, P. J. Cobalt Precursors for High-Throughput Discovery of Base Metal Asymmetric Alkene Hydrogenation Catalysts. *Science* **2013**, *342* (6162), 1076 – 1080.

(22) Palmer, W. N.; Diao, T.; Pappas, I.; Chirik, P. J. High-Activity Cobalt Catalysts for Alkene Hydroboration with Electronically Responsive Terpyridine and α-Diimine Ligands. *ACS Catal.* **2015**, *5* (2), 622–626.

(23) Léonard, N. G.; Chirik, P. J. Air-Stable α-Diimine Nickel Precatalysts for the Hydrogenation of Hindered, Unactivated Alkenes. *ACS Catal.* **2018**, *8* (1), 342–348.

(24) Schmidt, V. A.; Kennedy, C. R.; Bezdek, M. J.; Chirik, P. J. Selective [1,4]-Hydrovinylation of 1,3-Dienes with Unactivated Olefins Enabled by Iron Diimine Catalysts. *J. Am. Chem. Soc.* **2018**, *140* (9), 3443–3453.

(25) McNeill, E.; Ritter, T. 1,4-Functionalization of 1,3-Dienes With Low-Valent Iron Catalysts. *Acc. Chem. Res.* **2015**, *48* (8), 2330–2343.

(26) Moreau, B.; Wu, J. Y.; Ritter, T. Iron-Catalyzed 1,4-Addition of α-Olefins to Dienes. *Org. Lett.* **2009**, *11* (2), 337–339.

(27) Palmer, W. N.; Zarate, C.; Chirik, P. J. Benzyltriboronates: Building Blocks for Diastereoselective Carbon–Carbon Bond Formation. *J. Am. Chem. Soc.* **2017**, *139* (7), 2589–2592.

(28) Khusniyarov, M. M.; Weyhermüller, T.; Bill, E.; Wieghardt, K. Tuning the Oxidation Level, the Spin State, and the Degree of Electron Delocalization in Homo- and Heteroleptic Bis(α-Diimine)Iron Complexes. *J. Am. Chem. Soc.* **2009**, *131* (3), 1208–1221.

(29) Ghosh, M.; Sproules, S.; Weyhermüller, T.; Wieghardt, K. (α-Diimine)Chromium Complexes: Molecular and Electronic Structures; A Combined Experimental and Density Functional Theoretical Study. *Inorg. Chem.* **2008**, *47* (13), 5963–5970.

(30) Muresan, N.; Lu, C. C.; Ghosh, M.; Peters, J. C.; Abe, M.; Henling, L. M.; Weyhermüller, T.; Bill, E.; Wieghardt, K. Bis(α-Diimine)Iron Complexes: Electronic Structure Determination by Spectroscopy and Broken Symmetry Density Functional Theoretical Calculations. *Inorg. Chem.* **2008**, *47* (11), 4579–4590.

(31) Muresan, N.; Weyhermuller, T.; Wieghardt, K. Neutral Bis(1,4-Diaza-1,3-Butadiene)Nickel Complexes and Their Corresponding Monocations: Molecular and Electronic Structures. A Combined Experimental and Density Functional Theoretical Study. *Dalton Trans.* **2007**, No. 39, 4390–4398.

(32) Muresan, N.; Chlopek, K.; Weyhermüller, T.; Neese, F.; Wieghardt, K. Bis(α-Diimine)Nickel Complexes: Molecular and Electronic Structure of Three Members of the Electron-Transfer Series $[Ni(L)_2]^z$ (z = 0, 1+, 2+) (L = 2-Phenyl-1,4-Bis(Isopropyl)-1,4-Diazabutadiene). A Combined Experimental and Theoretical Study. *Inorg. Chem.* **2007**, *46* (13), 5327–5337.

(33) Lu, C. C.; Weyhermüller, T.; Bill, E.; Wieghardt, K. Accessing the Different Redox States of α-Iminopyridines within Cobalt Complexes. *Inorg. Chem.* **2009**, *48* (13), 6055–6064.

(34) van Gastel, M.; Lu, C. C.; Wieghardt, K.; Lubitz, W. Electron Paramagnetic Resonance and Electron Nuclear Double Resonance Investigation of the Diradical Bis(α-Iminopyridinato)Zinc Complex. *Inorg. Chem.* **2009**, *48* (6), 2626–2632.

(35) Römelt, C.; Weyhermüller, T.; Wieghardt, K. Structural Characteristics of Redox-Active Pyridine-1,6-Diimine Complexes: Electronic Structures and Ligand Oxidation Levels. *Coord. Chem. Rev.* **2019**, *380*, 287–317.

(36) Lundgren, R. J.; Stradiotto, M. Novel Catalysts, PCT/US2011 #061130, 2012.

(37) Borzenko, A.; Rotta-Loria, N. L.; MacQueen, P. M.; Lavoie, C. M.; McDonald, R.; Stradiotto, M. Nickel-Catalyzed Monoarylation of Ammonia. *Angew. Chemie Int. Ed.* **2015**, *54* (12), 3773–3777.

(38) Lundgren, R. J.; Peters, B. D.; Alsabeh, P. G.; Stradiotto, M. A P,N-Ligand for Palladium-Catalyzed Ammonia Arylation: Coupling of Deactivated Aryl Chlorides, Chemoselective Arylations, and Room Temperature Reactions. *Angew. Chemie Int. Ed.* **2010**, *49* (24), 4071–4074.

(39) Dub, P. A.; Scott, B. L.; Gordon, J. C. Air-Stable NNS (ENENES) Ligands and Their Well-Defined Ruthenium and Iridium Complexes for Molecular Catalysis. *Organometallics* **2015**, *34* (18), 4464–4479.

(40) Dub, P. A.; Scott, B. L.; Gordon, J. C. First-Row Transition Metal Complexes of ENENES Ligands: The Ability of the Thioether Donor to Impact the Coordination Chemistry. *Dalt. Trans.* **2016**, *45* (4), 1560–1571.

(41) O'Connor, C.; Lawlor, D. C.; Robinson, C.; Müller-Bunz, H.; Phillips, A. D. Comprehensive Experimental and Computational Study of H6-Arene Ruthenium(II) and Osmium(II) Complexes Supported by Sulfur Analogues of the β-Diketiminate Ligand. *Organometallics* **2018**, *37* (12), 1860–1875.

(42) Sriskandakumar, T.; Petzold, H.; Bruijnincx, P. C. A.; Habtemariam, A.; Sadler, P. J.; Kennepohl, P. Influence of Oxygenation on the Reactivity of Ruthenium−Thiolato Bonds in

Arene Anticancer Complexes: Insights from XAS and DFT. *J. Am. Chem. Soc.* **2009**, *131* (37), 13355–13361.

(43) Kandioller, W.; Hartinger, C. G.; Nazarov, A. A.; Kuznetsov, M. L.; John, R. O.; Bartel, C.; Jakupec, M. A.; Arion, V. B.; Keppler, B. K. From Pyrone to Thiopyrone Ligands−Rendering Maltol-Derived Ruthenium(II)−Arene Complexes That Are Anticancer Active in Vitro. *Organometallics* **2009**, *28* (15), 4249–4251.

(44) Bierenstiel, M.; Cross, E. D. Sulfur-Functionalized N-Heterocyclic Carbenes and Their Transition Metal Complexes. *Coord. Chem. Rev.* **2011**, *255* (5–6), 574–590.

(45) Huynh, H. V.; Yeo, C. H.; Tan, G. K. Hemilabile Behavior of a Thioether-Functionalized N-Heterocyclic Carbene Ligand. *Chem. Commun.* **2006**, No. 36, 3833–3835.

(46) Fliedel, C.; Schnee, G.; Braunstein, P. Versatile Coordination Modes of Novel Hemilabile S-NHC Ligands. *Dalton Trans.* **2009**, No. 14, 2474–2476.

(47) Huynh, H. V.; Yuan, D.; Han, Y. Syntheses and Catalytic Activities of Pseudo-Pincer and CSC Pincer-Type Pd(II) Complexes Derived from Benzannulated N-Heterocyclic Carbenes. *Dalton Trans.* **2009**, No. 35, 7262–7268.

(48) Yuan, D.; Tang, H.; Xiao, L.; Huynh, H. V. CSC-Pincer versus Pseudo-Pincer Complexes of Palladium(Ii): A Comparative Study on Complexation and Catalytic Activities of NHC Complexes. *Dalton Trans.* **2011**, *40* (35), 8788–8795.

(49) Bianchini, C.; Gatteschi, D.; Giambastiani, G.; Guerrero Rios, I.; Ienco, A.; Laschi, F.; Mealli, C.; Meli, A.; Sorace, L.; Toti, A.; et al. Electronic Influence of the Thienyl Sulfur Atom on the Oligomerization of Ethylene by Cobalt(II) 6-(Thienyl)-2-(Imino)Pyridine Catalysis. *Organometallics* **2007**, *26* (3), 726–739.

(50) Leipzig, B. K.; Rees, J. A.; Kowalska, J. K.; Theisen, R. M.; Kavčič, M.; Poon, P. C. Y.; Kaminsky, W.; DeBeer, S.; Bill, E.; Kovacs, J. A. How Do Ring Size and π-Donating Thiolate Ligands Affect Redox-Active, α-Imino-N-Heterocycle Ligand Activation? *Inorg. Chem.* **2018**, *57* (4), 1935–1949.

(51) Miller, P. E.; Oliver, G. L.; Dann, J. R.; Gates, J. W. By-Products of the Willgerodt Reaction Applied to α- and γ- Picoline. *J. Org. Chem.* **1957**, *22* (6), 664–666.

(52) Lindoy, L. F.; Livingstone, S. E. Reactions of Nickel Chelates Derived from 2-Aminobenzenethiol. *Inorg. Chem.* **1968**, *7* (6), 1149–1154.

(53) Lindoy, L. F.; Livingstone, S. E. Reactions of Copper Chelates Derived from 2-Aminobenzenethiol. *Inorganica Chim. Acta* **1968**, *2*, 166–168.

(54) Palmer, P. J.; Trigg, R. B.; Warrington, J. V. Benzothiazolines as Antituberculous Agents. *J. Med. Chem.* **1971**, *14* (3), 248–251.

(55) Capitán-Vallvey, L. F.; Espinosa, P. Rearrangement of 2-(2-Thienyl)Benzothiazoline in the Presence of Thiophilic Metal Ions. *Polyhedron* **1983**, *2* (11), 1147–1153.

(56) Chia, P. S. K.; Livingstone, S. E. Sulphur-Nitrogen Chelating Agents. VIII. Magnetic Behaviour of Some Cobalt(II) Complexes at the Crossover Region. *Aust. J. Chem.* **1969**, *22* (9), 1825–1833.

(57) Acosta-Ramirez, J. A.; Larade, M. C.; Lloy, S. M.; Cross, E. D.; McLellan, B. M.; Martell, J. M.; McDonald, R.; Bierenstiel, M. DFT and Experimental Study of the Structure and Vibrational Spectra of 2-(Benzylthio)-N-{pyridinylmethylidene}anilines. *J. Mol. Struct.* **2013**, *1034*, 29–37.

(58) Cross, E.; Shehzad, U.; Lloy, S.; Brown, A.; Mercer, T.; Foster, D.; McLellan, B.; Murray, A.; English, M.; Bierenstiel, M. Synthesis and Characterization of Donor-Functionalized N,S-Compounds Containing the Ortho-Aminothiophenol Motif. *Synthesis (Stuttg).* **2011**, *2011* (02), 303–315.

(59) Gonzalez, M. A.; Carrington, S. J.; Fry, N. L.; Martinez, J. L.; Mascharak, P. K. Syntheses, Structures, and Properties of New Manganese Carbonyls as Photoactive CO-Releasing Molecules: Design Strategies That Lead to CO Photolability in the Visible Region. *Inorg. Chem.* **2012**, *51* (21), 11930–11940.

(60) Martin, D. J.; McCarthy, B. D.; Piro, N. A.; Dempsey, J. L. Synthesis and Electrochemical Characterization of a Tridentate Schiff-Base Ligated Fe(II) Complex. *Polyhedron* **2016**, *114*, 200–204. (61) Chatterjee, S. K.; Maji, R. C.; Barman, S. K.; Olmstead, M. M.; Patra, A. K. Hexacoordinate Nickel(II)/(III) Complexes That Mimic the Catalytic Cycle of Nickel Superoxide Dismutase. *Angew. Chemie* **2014**, *126* (38), 10348–10353.

(62) Chatterjee, S. K.; Roy, S.; Barman, S. K.; Maji, R. C.; Olmstead, M. M.; Patra, A. K. Shuttling of Nickel Oxidation States in N_4S_2 Coordination Geometry versus Donor Strength of Tridentate N_2S Donor Ligands. *Inorg. Chem.* **2012**, *51* (14), 7625–7635.

(63) Maji, M.; Hossain, M.; Chatterjee, M.; Chattopadhyay, S. K.; Puranik, V. G.; Chakrabarti, P.; Ghosh, S. Synthesis, Characterisation and Reactivity of Trans-[Ru(L)(PPh_3)Br_2]; L=2-Pyridyl-N-(2′-Methylthiophenyl)Methyleneimine: Crystal Structure of Trans-[Ru(L)(PPh_3)Br_2]. *Polyhedron* **1999**, *18* (27), 3735–3739.

(64) Hossain, M.; Maji, M.; Chattopadhyay, S. K.; Ghosh, S.; Blake, A. J. Synthesis, Characterization and Reactivity of Cis-Ru (L)(PPh_3) Cl_2; L = 2-Pyridyl-N-(2′-Methylthiophenylmethyleneimine) Crystal Structure of Cis-Ru(L)(PPh_3)Cl_2 and [Ru(L)(PPh_3)(Bpy)](ClO_4)$_2$. *Polyhedron* **1998**, *17* (11), 1897–1906.

(65) Udo, B.; Heinrich, V. Zinc Complexes of the N,N,S Ligand (Mercaptophenyl)(Picolyl)Amine. *Chem. Ber. 129* (4), 435–440.

(66) Tyler, L. A.; Noveron, J. C.; Olmstead, M. M.; Mascharak, P. K. Co(III) Complexes with Coordinated Carboxamido Nitrogens and Thiolato Sulfurs as Models for Co-Containing Nitrile Hydratase and Their Conversion to the Corresponding Sulfinato Species. *Inorg. Chem.* **2000**, *39* (2), 357–362.

(67) Gonzalez, M. A.; Carrington, S. J.; Chakraborty, I.; Olmstead, M. M.; Mascharak, P. K. Photoactivity of Mono- and Dicarbonyl Complexes of Ruthenium(II) Bearing an N,N,S-Donor Ligand: Role of Ancillary Ligands on the Capacity of CO Photorelease. *Inorg. Chem.* **2013**, *52* (19), 11320–11331.

(68) Lee, D. G.; Wang, Z.; Chandler, W. D. Autocatalysis during the Reduction of Tetra-n-Propylammonium Perruthenate by 2-Propanol. *J. Org. Chem.* **1992**, *57* (12), 3276–3277.

(69) Chandler, W. D.; Wang, Z.; Lee, D. G. Kinetics and Mechanism of the Oxidation of Alcohols by Tetrapropylammonium Perruthenate. *Can. J. Chem.* **2005**, *83* (9), 1212–1221.

(70) Zerk, T. J.; Moore, P. W.; Williams, C. M.; Bernhardt, P. V. N-Oxides Rescue Ru(v) in Catalytic Griffith–Ley (TPAP) Alcohol Oxidations. *Chem. Commun.* **2016**, *52* (67), 10301–10304.

(71) Zerk, T. J.; Moore, P. W.; Harbort, J. S.; Chow, S.; Byrne, L.; Koutsantonis, G. A.; Harmer, J. R.; Martínez, M.; Williams, C. M.; Bernhardt, P. V. Elucidating the Mechanism of the Ley–Griffith (TPAP) Alcohol Oxidation. *Chem. Sci.* **2017**, *8* (12), 8435–8442.

(72) Singh, P.; Singh, A. K. Transfer Hydrogenation of Ketones and Catalytic Oxidation of Alcohols with Half-Sandwich Complexes of Ruthenium(II) Designed Using Benzene and Tridentate (S, N, E) Type Ligands (E = S, Se, Te). *Organometallics* **2010**, *29* (23), 6433–6442.

(73) McSkimming, A.; Bhadbhade, M. M.; Colbran, S. B. Synthesis and (Spectro)Electrochemical Investigations of Coordinatively-Saturated (Cyclopentadienyl)Ruthenium–Hantzsch Pyridinium/Dihydropyridine Conjugates. *Inorganica Chim. Acta* **2016**, *444*, 103–112.

(74) Gichumbi, J. M.; Friedrich, H. B.; Omondi, B. Synthesis and Characterization of Some New Half-Sandwich Ruthenium(II) Complexes with Bidentate N , N ′-Ligands and Their Application in Alcohol Oxidatio. *Inorganica Chim. Acta* **2017**, *456*, 55–63.

(75) Hunter, A. D.; Williams, T. R.; Zarzyczny, B. M.; Bottesch, H. W.; Dolan, S. A.; McDowell, K. A.; Thomas, D. N.; Mahler, C. H. Correlations among 31P NMR Coordination Chemical Shifts, Ru–P Bond Distances, and Enthalpies of Reaction in Cp′Ru(PR_3)$_2$Cl Complexes (Cp′ = η^5-C_5H_5, η^5-C_5Me_5; PR_3 = PMe_3, $PPhMe_2$, PPh_2Me, PPh_3, PEt_3, $PnBu_3$). *Organometallics* **2016**, *35* (16), 2701–2706.

(76) Bratsos, I.; Alessio, E. The Pivotal Role of Ru-Dmso Compounds in the Discovery of Well-Behaved Precursors. *Eur. J. Inorg. Chem.* **2018**, *2018* (26), 2996–3013.

(77) Ogweno, A. O.; Ojwach, S. O.; Akerman, M. P. (Pyridyl)Benzoazole Ruthenium(Ii) and Ruthenium(Iii) Complexes: Role of Heteroatom and Ancillary Phosphine Ligand in the Transfer Hydrogenation of Ketones. *Dalt. Trans.* **2014**, *43* (3), 1228–1237.

(78) Krogh-Jespersen, K.; Zhang, X.; Westbrook, J. D.; Fikar, R.; Nayak, K.; Kwik, W. L.; Potenza, J. A.; Schugar, H. J. Crystal, Molecular, and Electronic Structures of Pentaammineruthenium(III)-Thioether Complexes. *J. Am. Chem. Soc.* **1989**, *111* (11), 4082–4091.

(79) Gorelsky, S.; Lever, A.; Ebadi, M. Ruthenium D-Orbital Delocalization in Bis(Bipyridine)Ruthenium Derivatives of Redox Active Quinonoid Ligand. *Coord. Chem. Rev.* **2002**, *230* (1–2), 97–105.

Supporting Information

Ruthenium(II) complexes bearing thioether-appended α-iminopyridine ligands: Arene precursors permit access to κ^2-N,N and κ^3-N,N,S complexes

Ternes, Victoria A.; Morgan, Hannah A.; Lanquist, Austin P.; Murray, Michael J.; Wile, Bradley M.*

Donald J. Bettinger Department of Chemistry and Biochemistry, Ohio Northern University, 525 South Main Street, Ada, OH 45810, USA

*Author to whom correspondence should be addressed: b-wile@onu.edu (419) 772-2986

Contents

Table S1. Crystallographic data for **[1-RuCl(NCMe)$_2$] Cl**

Compound	**[1-RuCl(NCMe)$_2$] Cl · 3 H$_2$O**
empirical formula	$C_{17}H_{18}Cl_2N_4RuS \cdot 3\ H_2O$
formula weight	536.43
crystal size	0.42 × 0.15 × 0.05
crystal system	triclinic
space group	P_{-1}
a (Å)	7.8414(3)
b (Å)	9.9955(4)
c (Å)	14.6972(6)
α (deg)	79.0934(16)
β (deg)	85.2301(16)
γ (deg)	78.5490(16)
V (Å^3)	1107.38(8)
Z	2
ρ_{cacld} (g cm^{-1})	1.609
μ (mm^{-1})	1.07
F(000)	544
Radiation	MoK$_\alpha$ (λ = 0.71073)
2θ limit (deg)	2.947 to 36.347
	$-11 \le h \le 13$
	$-16 \le k \le 16$
	$-24 \le l \le 24$
total data collected	49003
number of independent reflections	10706
number of observed reflections	8557
R_{int}	0.041
abs correction	Multiscan (SADABS)
range of transmission	0.6536 – 0.7471
data/restraints/params	10706/22/317
R_1 [$F_o^2 \ge 2\sigma(F_o^2)$]	0.0440
wR_2 [$F_o^2 \ge -3\sigma(F_o^2)$]	0.0989
GOF	1.094
Largest peak/hole (e Å^{-3})	3.221/-1.605

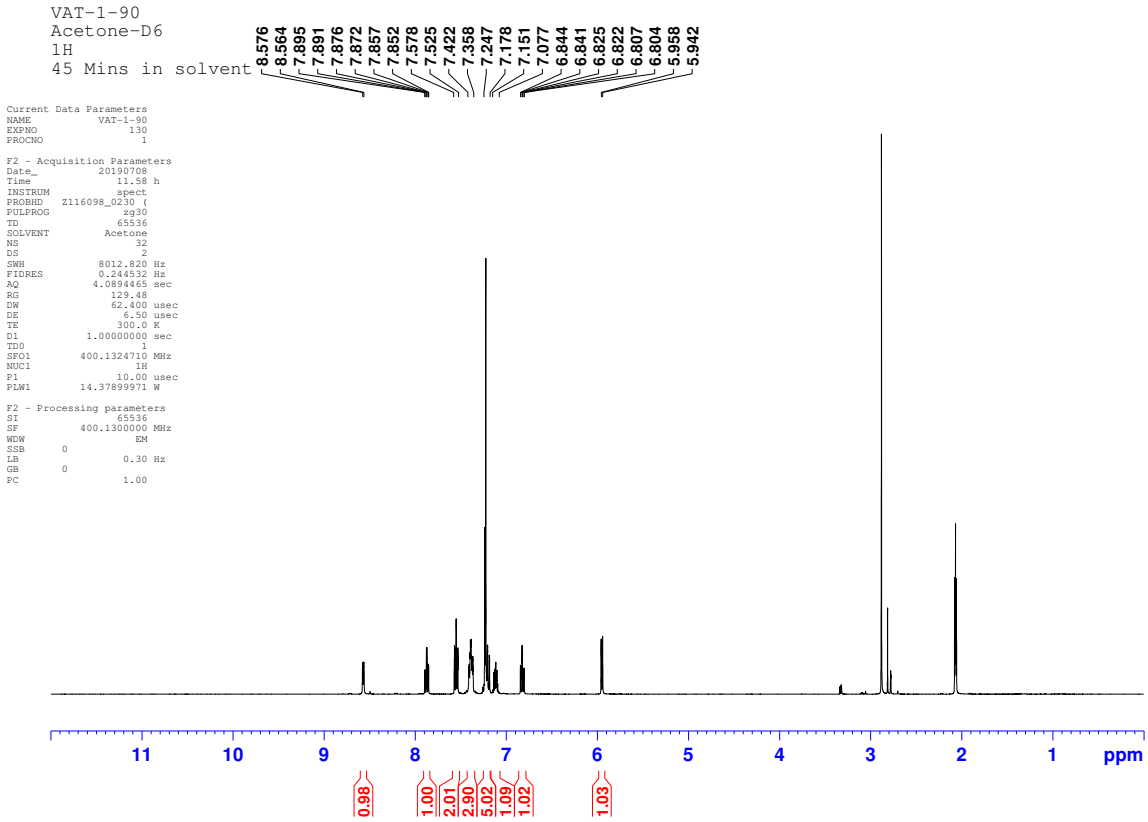

Figure S1 – ^{1}H NMR spectrum of **3**

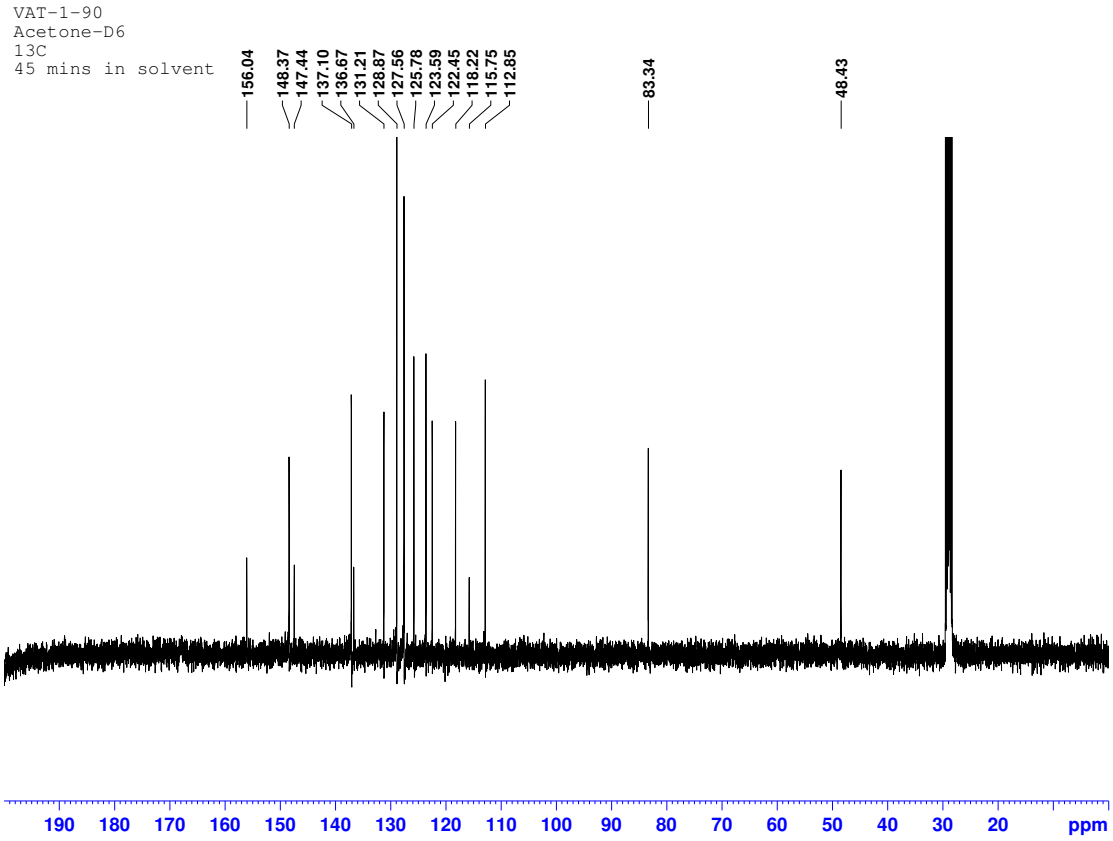

Figure S2 – ^{13}C NMR spectrum of **3**

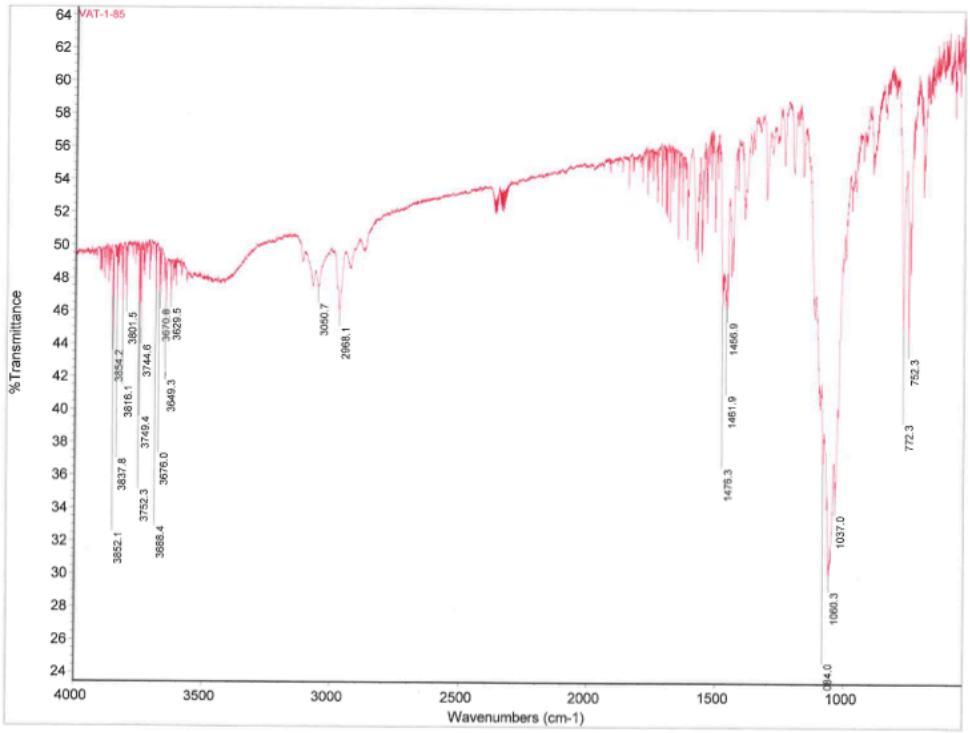

Figure S3 – IR spectrum of **3**

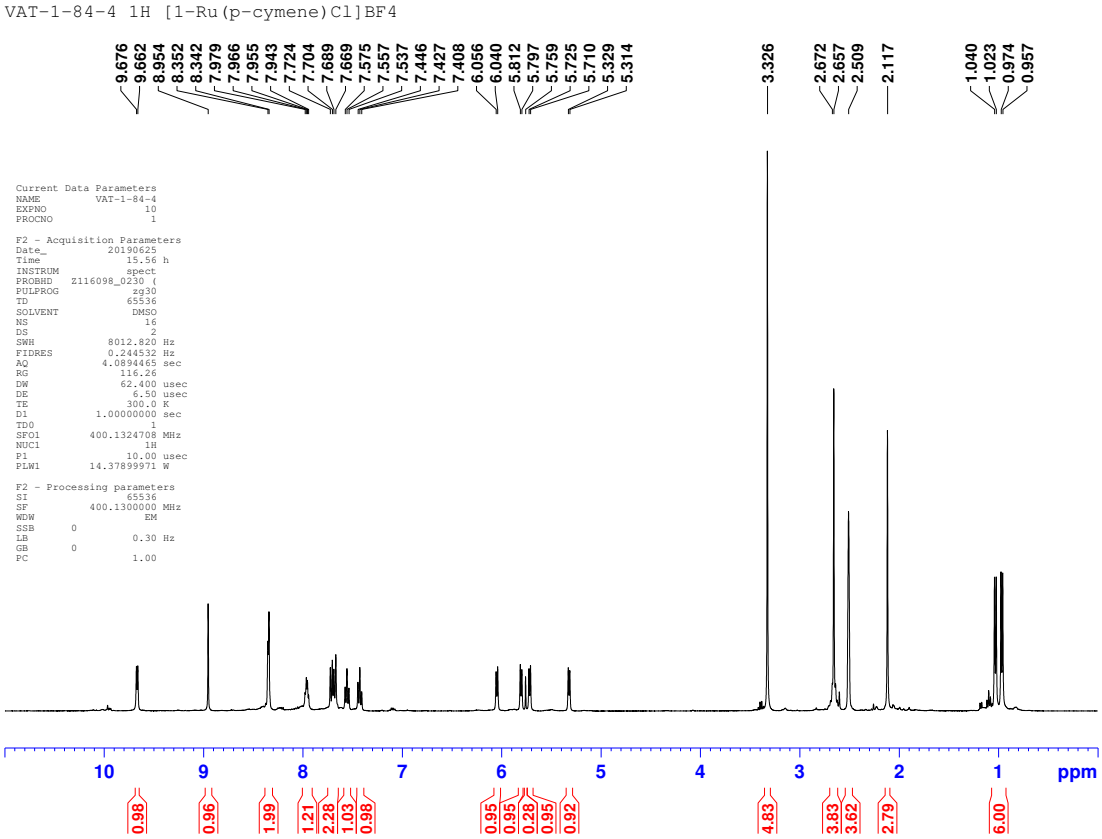

Figure S4 – ^{1}H NMR spectrum of **[1-Ru(p-cymene)Cl] BF_4**

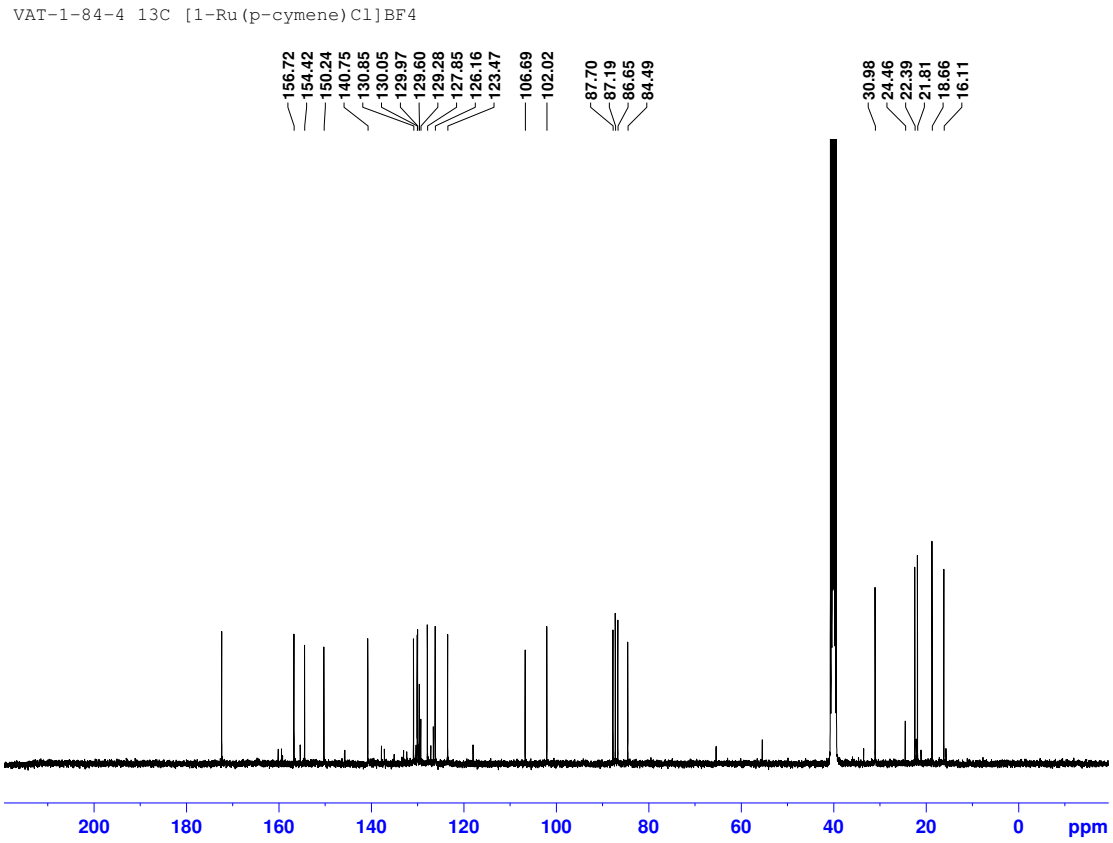

Figure S5 – ^{13}C NMR spectrum of **[1-Ru(p-cymene)Cl] BF_4**

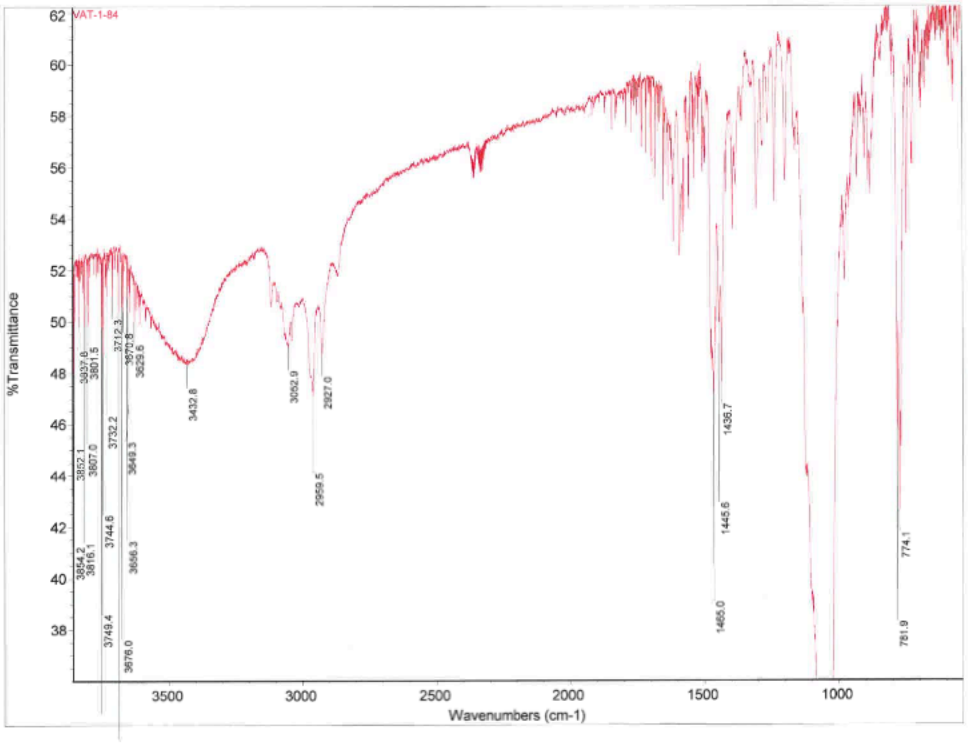

Figure S6 – IR spectrum of **[1-Ru(p-cymene)Cl] BF_4**

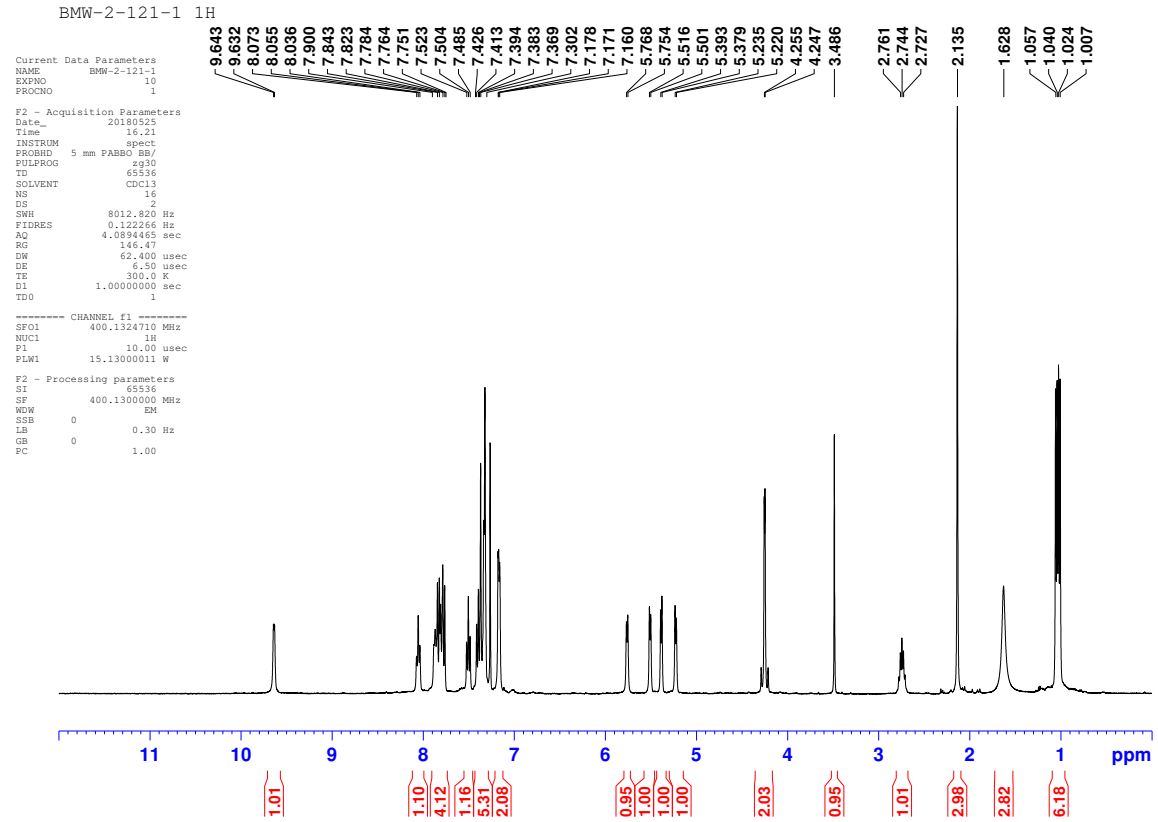

Figure S7 – ^{1}H NMR spectrum of **[2-Ru(p-cymene)Cl] BF_4**

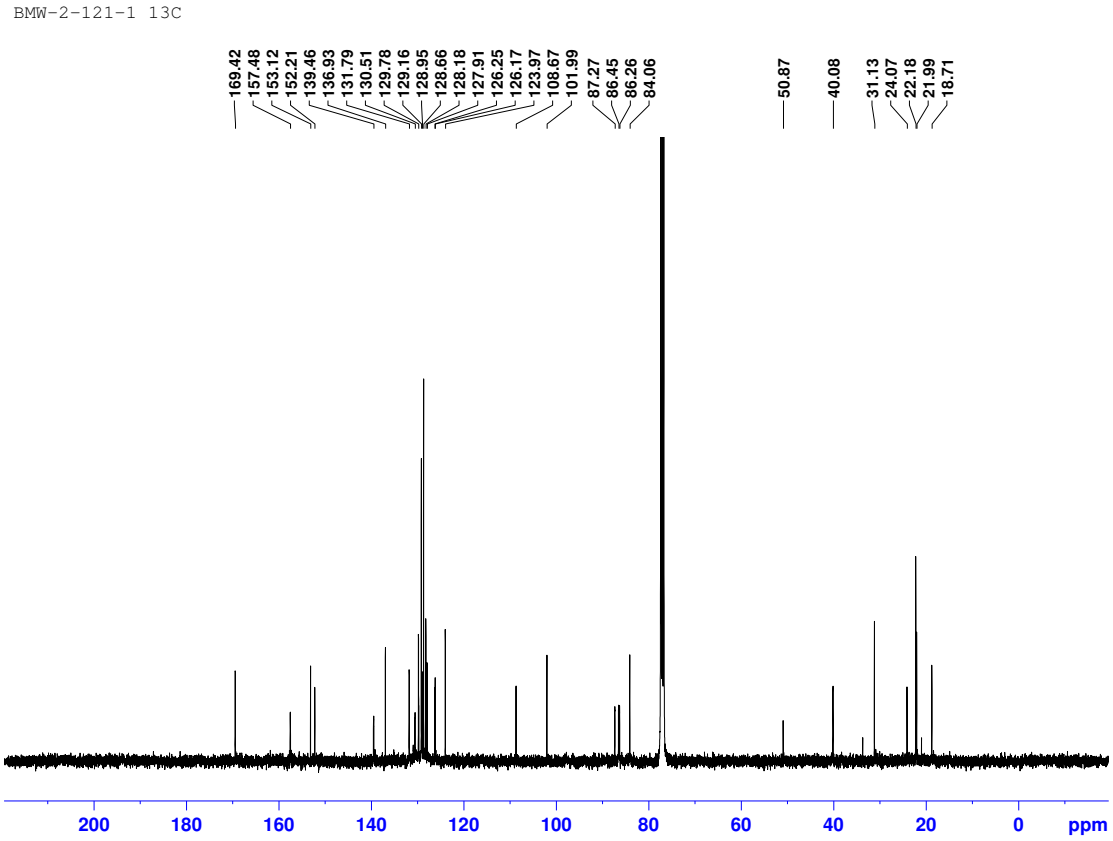

Figure S8 – ^{13}C NMR spectrum of **[2-Ru(p-cymene)Cl] BF_4**

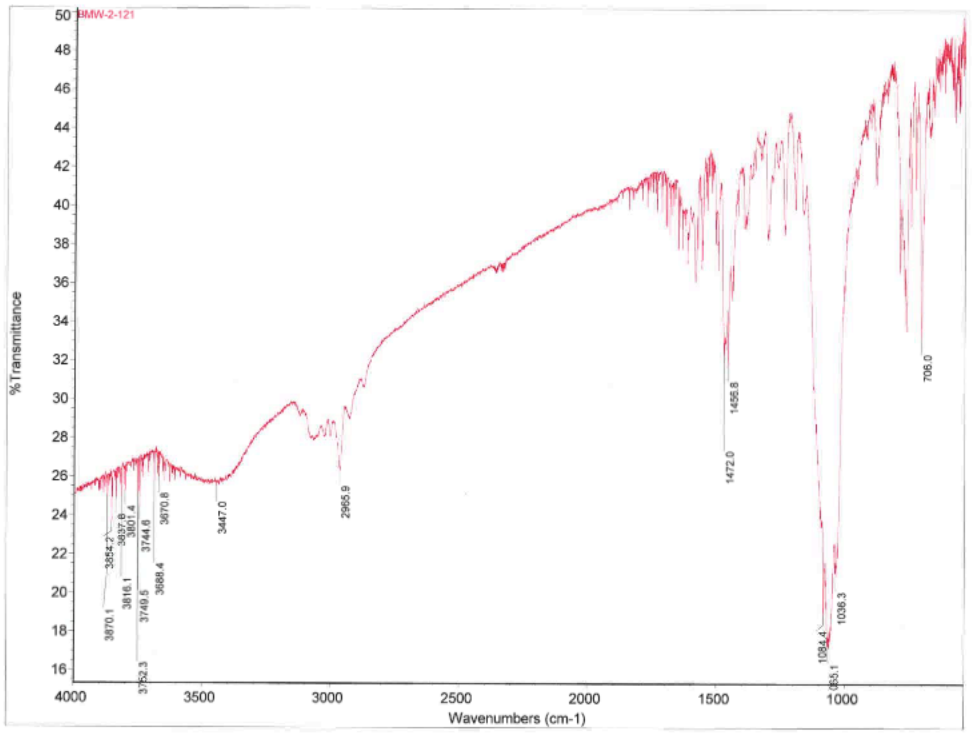

Figure S9 – IR spectrum of **[2-Ru(p-cymene)Cl] BF_4**

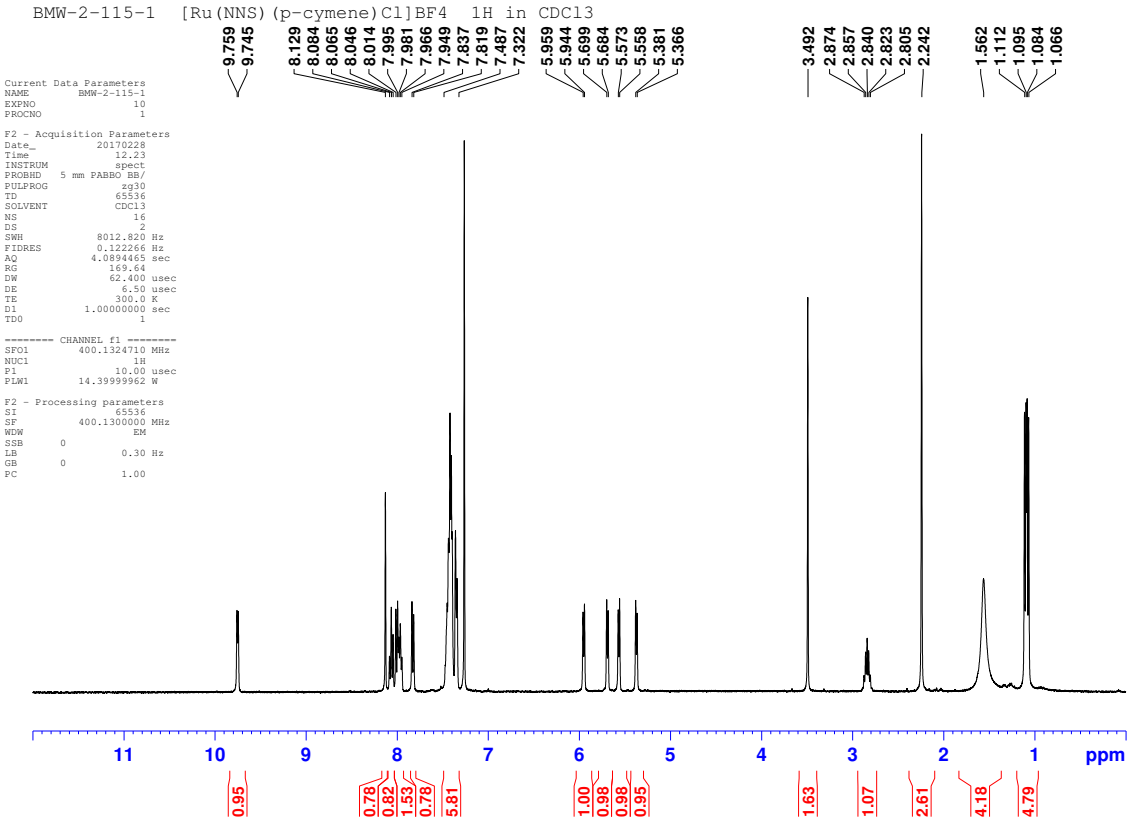

Figure S10 – ^{1}H NMR spectrum of **[3-Ru(p-cymene)Cl] BF_4**

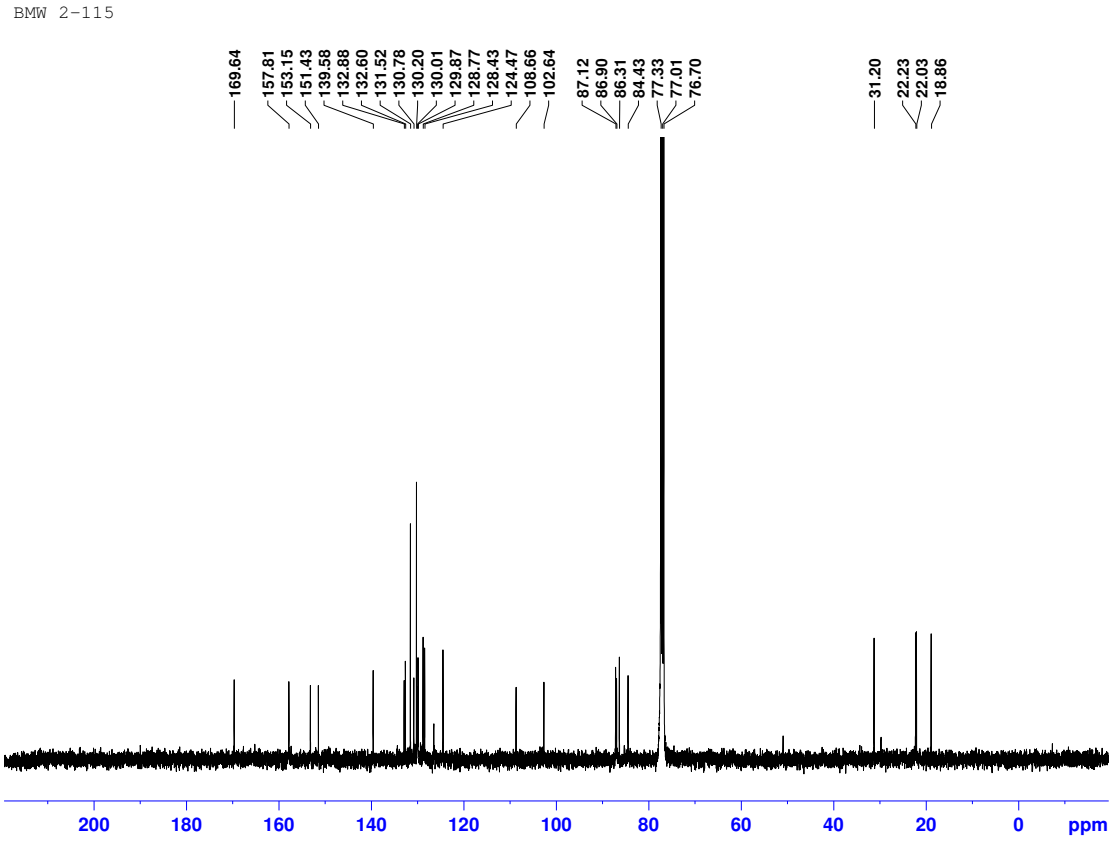

Figure S11 – ^{13}C NMR spectrum of **[3-Ru(p-cymene)Cl] BF_4**

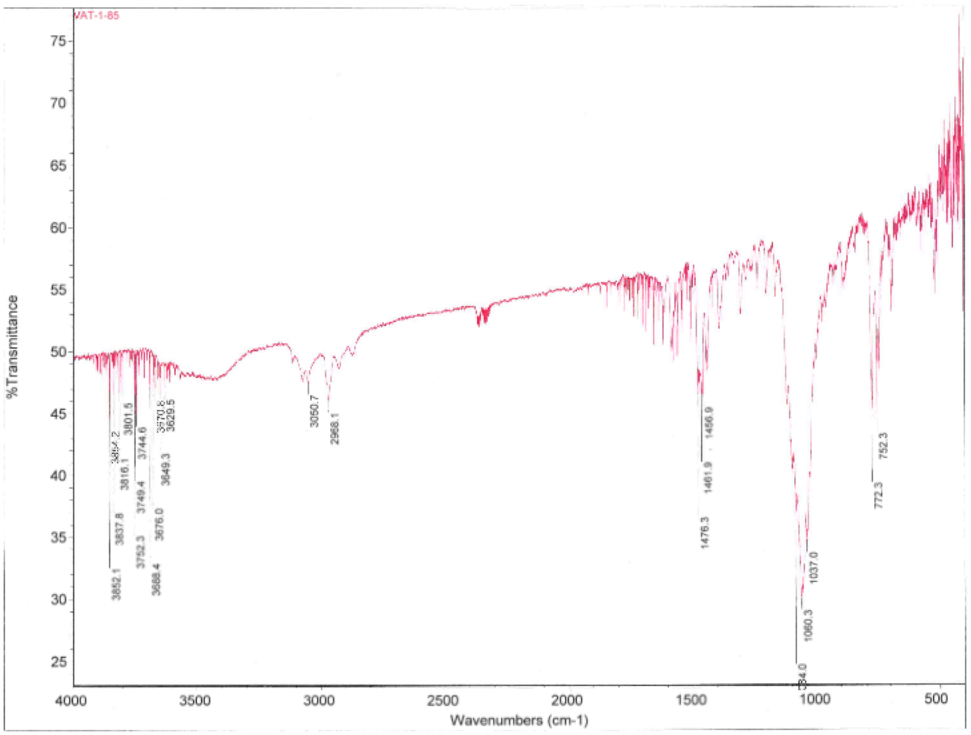

Figure S12 – IR spectrum of **[3-Ru(p-cymene)Cl] BF_4**

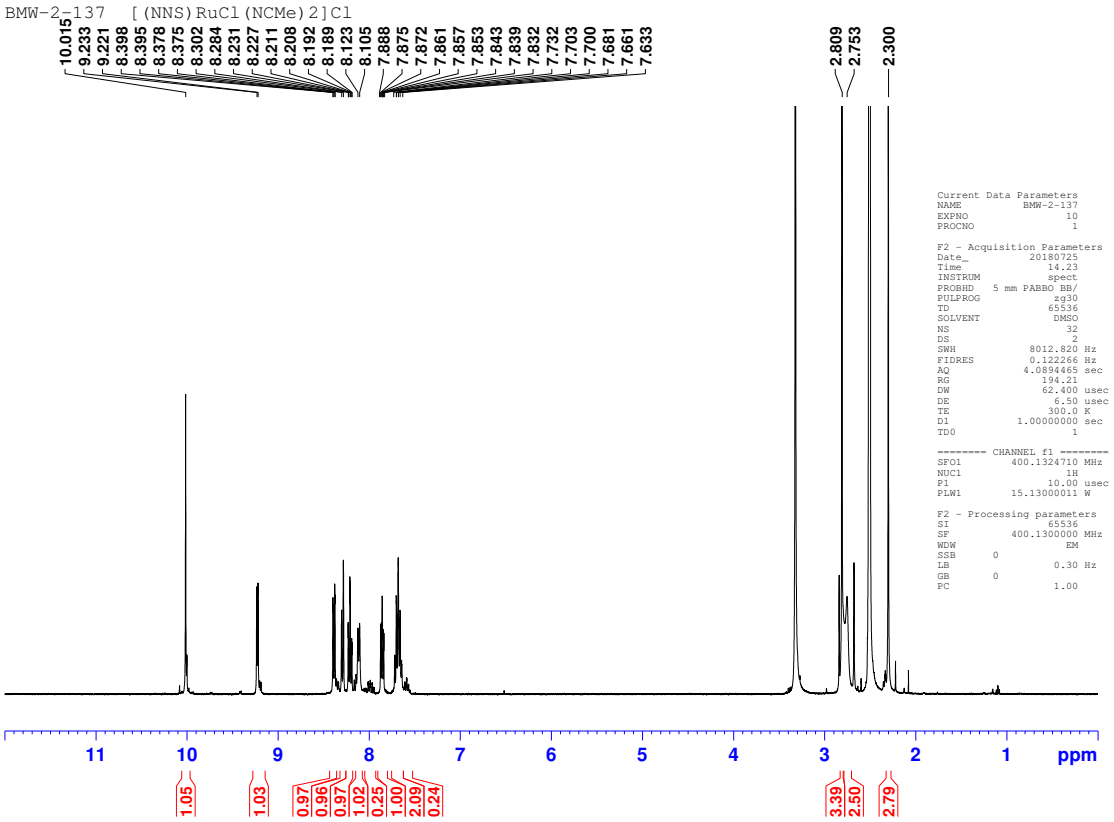

Figure S13 – ^{1}H NMR spectrum of **[1-RuCl(NCMe)$_2$] Cl**

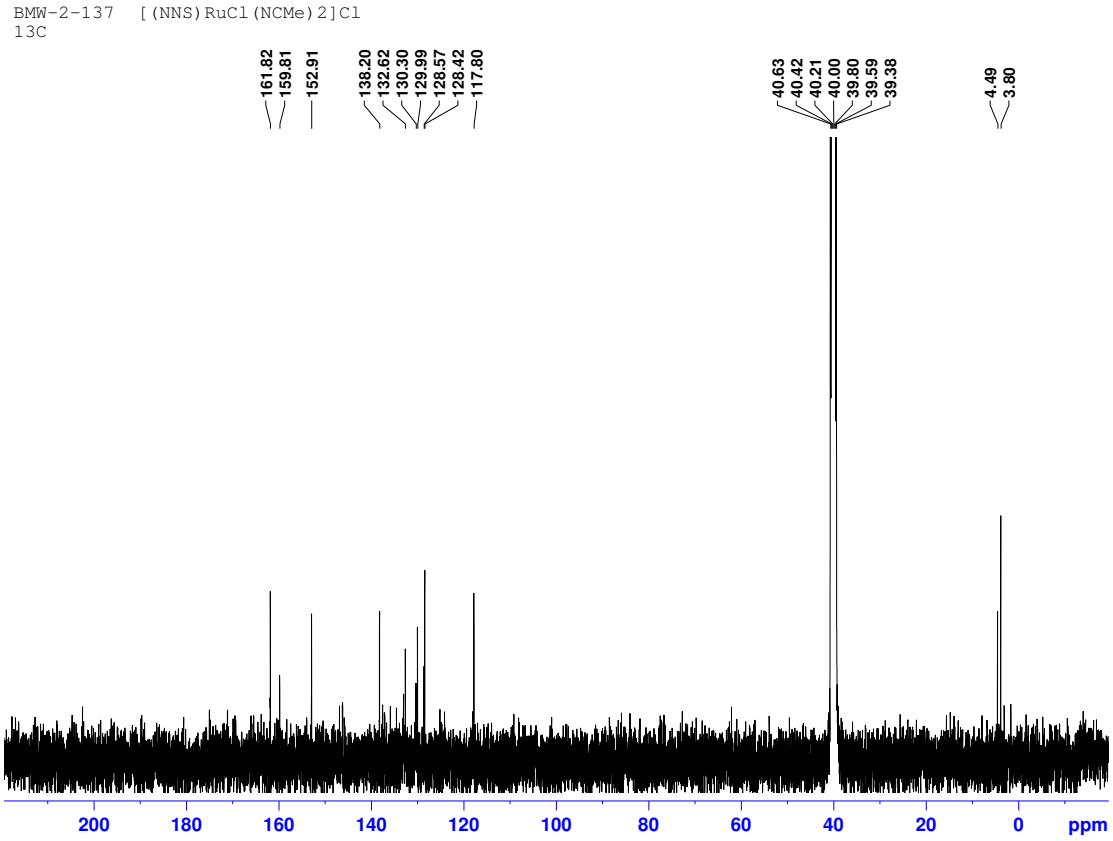

Figure S14 – ^{13}C NMR spectrum of **[1-RuCl(NCMe)$_2$] Cl**

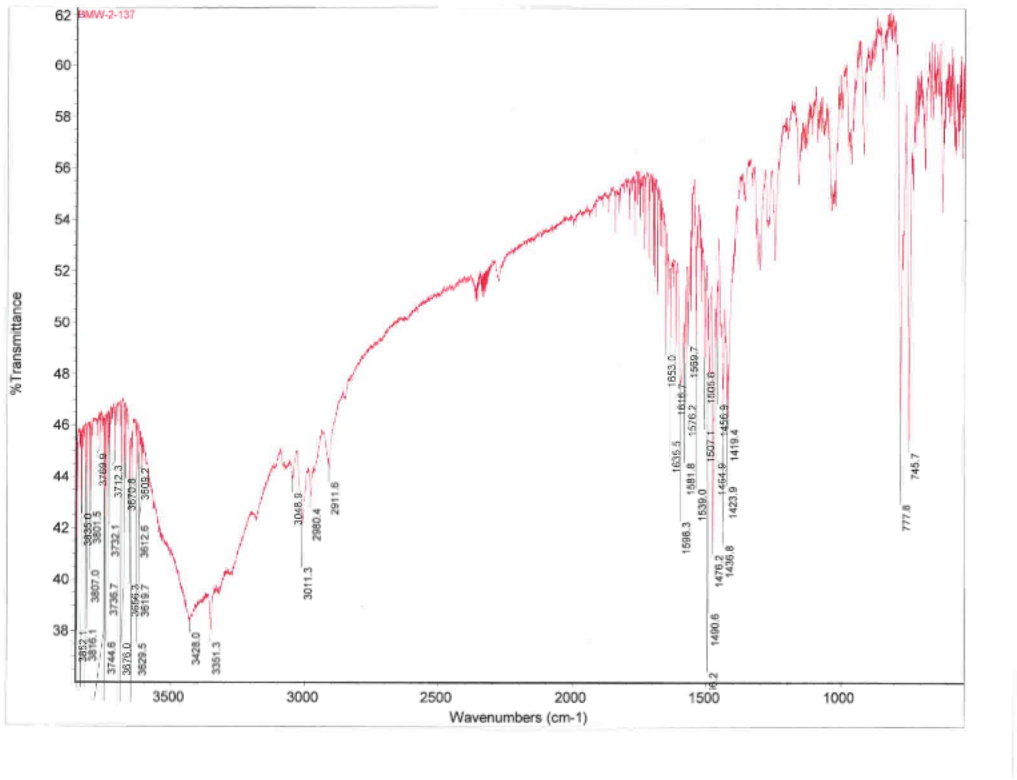

Figure S15 – IR spectrum of **[1-RuCl(NCMe)$_2$] Cl**